$O(\alpha_s)$ corrections to the polar angle dependence of the longitudinal spin-spin correlation asymmetry in $e^+e^- \to q\bar{q}$

S. Groote, J.G. Körner and J.A. Leyva

Institut für Physik, Johannes-Gutenberg-Universität,

Staudinger Weg 7, 55099 Mainz, Germany

Abstract

We provide analytical results for the $O(\alpha_s)$ corrections to the polar angle dependence of the longitudinal spin-spin correlation asymmetry in $e^+e^- \to q\bar{q}$. For top quark pair production the $O(\alpha_s)$ corrections to the longitudinal spin-spin asymmetry are strongly polar angle dependent and can amount up to $\simeq 4\%$ in the q^2-range from above $t\bar{t}$-threshold up to $\sqrt{q^2} = 1000\,\mathrm{GeV}$. The $O(\alpha_s)$ radiative corrections to the correlation asymmetry are below $\approx 1\%$ in the forward direction where the cross section is largest. In the $e^+e^- \to b\bar{b}$ case the $O(\alpha_s)$ corrections reduce the asymmetry value from its $m_b = 0$ value of -100% to approximately -96% for q^2-values around the Z peak and are practically independent of the value of the polar angle θ. This reduction can be traced to finite anomalous contributions from residual mass effects which survive the $m_b \to 0$ limit. We discuss the role of the anomalous contributions and the pattern of how they contribute to spin-flip and non-flip terms.

1 Introduction

Since polarized top and antitop quarks decay weakly before hadronizing they retain their original polarization from the production process when they decay. There are thus significant correlations between the decay products of jointly produced top and antitop quarks. The relevant spin information is encoded in the spin-spin density matrix of the $(t\bar{t})$-system. For hadronically produced $(t\bar{t})$-pairs such correlations have been thoroughly discussed in the review article [1]. In $e^+e^- \to t\bar{t}$ interactions the spin-spin density matrix of the $(t\bar{t})$-system [2, 3, 4, 5, 6, 7] and the ensuing correlations between the decay products [2, 3] have been studied in a number of papers.

Of interest is also the role of quark mass effects in the production of quarks and gluons in e^+e^--annihilations. Jet definition schemes, event shape variables, heavy flavour momentum correlations [8, 9, 10] and the polarization of the gluon [11] are affected by the presence of quark masses for charm and bottom quarks even when they are produced at the scale of the Z^0 mass. A careful investigation of quark mass effects in e^+e^--annihilations may even lead to an alternative determination of the quark mass values [8, 9, 10, 12]. There is an obvious interest in quark mass effects for $(t\bar{t})$-production where quark mass effects cannot be neglected in the envisaged range of energies to be covered by the proposed International Linear Collider (ILC). At the low mass end quark mass effects are important in the $m_q \to 0$ calculation of radiative corrections to quark polarization variables because residual mass effects change the naive non-flip pattern of the $m_q = 0$ polarization results [13, 14]. In QED the same $O(\alpha/\pi)$ residual mass effects have been widely discussed in polarized lepton production [15, 16, 17] and polarization effects in lepton decays [18, 19, 20].

In this report we provide analytical results for the $O(\alpha_s)$ radiative corrections to the longitudinal spin-spin correlation asymmetry (called longitudinal spin-spin asymmetry for short) and its polar angle dependence for massive quark pairs produced in e^+e^--annihilations. This goes beyond the calculation of Ref. [5, 6] where the polar angle dependence was averaged over. In contrast to the analysis [7], which was numerical, our results are presented in closed analytic form which allows one to explicitly study the high energy (or $m_q \to 0$) limit of the relevant spin-spin density matrix elements which differ from the naive $m_q = 0$ values due to the residual quark mass effects.

The longitudinal polarization of massive quark pairs produced in e^+e^--interactions affects the shape of the energy spectrum of their secondary decay leptons. For example, the longitudinal spin-spin correlation effects in pair produced top quarks and antitop quarks will lead to correlation effects of the energy spectra of their secondary decay leptons and antileptons. We discuss in detail the $m_q \to 0$ limit of the relevant polarized structure functions and the role of the $O(\alpha_s)$ residual mass effects which are mostly relevant for charm and bottom quarks for energies at and above the Z and for top quarks at the highest energy $\sqrt{q^2} = 1000\,\text{GeV}$. We delineate how residual mass effects contribute to the various spin-flip and non-flip terms in the $m_q \to 0$ limit for each of the three spin-spin correlation functions that describe the polar angle dependence of the longitudinal spin-spin correlations.

2 Joint quark-antiquark density matrix and polar angle distribution

Let us begin by defining the differential joint quark-antiquark density matrix $d\boldsymbol{\sigma}^\alpha = d\sigma^\alpha_{\lambda_1\lambda_2;\lambda'_1\lambda'_2}$ where λ_1 (λ'_1) and λ_2 (λ'_2) denote the helicities of the quark and antiquark, respectively. The label α specifies the polarization of the initial γ^* and Z, or interference contributions thereof, which determines the polar angle dependence of the cross section and the longitudinal spin-spin correlations. In our notation the three polarization components are called $\alpha = U$ (unpolarized transverse), L (longitudinal) and F (forward–backward).

In this paper we concentrate on the longitudinal polarization of the quark and antiquark, and in particular, on their longitudinal spin-spin correlations. Thus we specify to the diagonal case $\lambda_1 = \lambda'_1$ and $\lambda_2 = \lambda'_2$. The diagonal part of the differential joint density matrix can be represented in terms of its components along the products of the unit matrix $\mathbb{1}$ and the z-components of the Pauli matrix $\boldsymbol{\sigma}_3$ ($\boldsymbol{\sigma}_3 = \hat{p}_1\vec{\sigma}$ for the quark and $\boldsymbol{\sigma}_3 = \hat{p}_2\vec{\sigma}$ for the antiquark, $\hat{p}_i = \vec{p}_i/|\vec{p}_i|$). One has

$$d\boldsymbol{\sigma}_\alpha = \frac{1}{4}\left(\sigma_\alpha \mathbb{1}\otimes\mathbb{1} + \sigma^{(\ell_1)}_\alpha \boldsymbol{\sigma}_3\otimes\mathbb{1} + \sigma^{(\ell_2)}_\alpha \mathbb{1}\otimes\boldsymbol{\sigma}_3 + \sigma^{(\ell_1\ell_2)}_\alpha \boldsymbol{\sigma}_3\otimes\boldsymbol{\sigma}_3\right), \tag{1}$$

where the Pauli matrices to the left and right of the $\otimes$ symbol are associated with the quark and the antiquark, respectively.

In order to get a feeling about the physical significance of the single and double spin functions $\sigma^{(\ell_{1,2})}_\alpha$ and $\sigma^{(\ell_1\ell_2)}_\alpha$ consider the case where the polarization of the quarks and antiquarks is purely longitudinal in the helicity system. This would be the case in the high energy limit since the transverse spin components of the top and antitop quark go to zero as $m_q/\sqrt{q^2}$. The differential distribution with respect to the polar angles $\cos\theta_{1,2}$ specifying the angles between the (quark, antiquark) and given decay products thereof reads

$$\frac{d\sigma_\alpha}{d\cos\theta_1 d\cos\theta_2} = \frac{1}{4}\Big(\sigma_\alpha + \sigma^{(\ell_1)}_\alpha \alpha_1\cos\theta_1 + \sigma^{(\ell_2)}_\alpha \alpha_2\cos\theta_2$$
$$+ \sigma^{(\ell_1\ell_2)}_\alpha \alpha_1\alpha_2\cos\theta_1\cos\theta_2\Big), \tag{2}$$

where the asymmetry parameters $\alpha_{1,2}$ specify the analyzing power of the particular final state in the respective decay channels. Consider, for example, $(t\bar{t})$-production followed by the semileptonic decays $t \to b + \ell^+ + \nu_\ell$ and $\bar{t} \to \bar{b} + \ell^- + \bar{\nu}_\ell$. Each of the decay products of the top and antitop can serve as a polarization analyzer of the spin of the top and antitop quarks. From the experimental point of view the charged leptons $\ell^\pm$ are ideally suited for this purpose because they are easy to detect and because their analyzing power is maximal with $\alpha_{1,2} = \pm 1$ (see e.g. [21]).

An alternative but equivalent representation of the longitudinal spin contributions in Eq. (1) can be written down for the double density matrix elements $\sigma_\alpha(s^\ell_1, s^\ell_2)$ in terms of the longitudinal spin components $s^\ell_1 = 2\lambda_1$ and $s^\ell_2 = 2\lambda_2$ with $s^\ell_1, s^\ell_2 = \pm 1$ (or $s^\ell_1, s^\ell_2 \in \{\uparrow,\downarrow\}$). One has

$$\sigma_\alpha(s^\ell_1, s^\ell_2) = \frac{1}{4}\left(\sigma_\alpha + \sigma^{(\ell_1)}_\alpha s^\ell_1 + \sigma^{(\ell_2)}_\alpha s^\ell_2 + \sigma^{(\ell_1\ell_2)}_\alpha s^\ell_1 s^\ell_2\right). \tag{3}$$

Eq. (3) is easily inverted. The result is

$$
\begin{aligned}
\sigma_\alpha &= \sigma_\alpha(\uparrow\uparrow) + \sigma_\alpha(\uparrow\downarrow) + \sigma_\alpha(\downarrow\uparrow) + \sigma_\alpha(\downarrow\downarrow), \\
\sigma_\alpha^{(\ell_1)} &= \sigma_\alpha(\uparrow\uparrow) + \sigma_\alpha(\uparrow\downarrow) - \sigma_\alpha(\downarrow\uparrow) - \sigma_\alpha(\downarrow\downarrow), \\
\sigma_\alpha^{(\ell_2)} &= \sigma_\alpha(\uparrow\uparrow) - \sigma_\alpha(\uparrow\downarrow) + \sigma_\alpha(\downarrow\uparrow) - \sigma_\alpha(\downarrow\downarrow), \\
\sigma_\alpha^{(\ell_1\ell_2)} &= \sigma_\alpha(\uparrow\uparrow) - \sigma_\alpha(\uparrow\downarrow) - \sigma_\alpha(\downarrow\uparrow) + \sigma_\alpha(\downarrow\downarrow).
\end{aligned}
\tag{4}
$$

In the following we shall refer to the $(\uparrow\downarrow)$ and $(\downarrow\uparrow)$ spin configurations as aligned even if the quark and antiquark are not parallel.

$O(\alpha_s)$ radiative corrections to the unpolarized rate components σ_α have been discussed before (see e.g. [13, 14, 22]) including beam polarization effects [14] and beam-event correlation effects [14, 22]. The $O(\alpha_s)$ radiative corrections to the longitudinal spin component $\sigma_{U+L}^{(\ell_1)}$ (and thereby $\sigma_{U+L}^{(\ell_2)}$) have been calculated in Refs. [13, 23]. Beam polarization and $O(\alpha_s)$ beam-event correlation effects for $\sigma_\alpha^{(\ell_1)}$ ($\alpha = U, L, F$) were calculated in [14, 24, 25]. As concerns the spin-spin correlation asymmetry $\sigma_\alpha^{(\ell_1\ell_2)}$ the $O(\alpha_s)$ tree graph contributions have been written down in Ref. [4]. The complete $O(\alpha_s)$ radiative corrections to the fully integrated spin-spin correlation component $\sigma_{U+L}^{(\ell_1\ell_2)}$ were calculated in Refs. [5, 6] where beam-event correlation effects were averaged over. These results were confirmed in a numerical calculation by Brandenburg $et\ al.$ [7]. As mentioned in the introduction to this paper we are aiming to determine the polar angle dependence of the longitudinal spin-spin correlation asymmetry, i.e. we are interested in the polar angle structure induced by the rate functions σ_α and the longitudinal spin-spin functions $\sigma_\alpha^{(\ell_1\ell_2)}$ ($\alpha = U, L, F$).

As before we write the electroweak cross section and the spin-spin correlation components in modular form in terms of three building blocks [14], namely the lepton tensor (which encapsules the beam polarization parameters and the angular dependences), the hadron tensor (which contains the hadron dynamics) and an electroweak coupling matrix $g_{ij}(q^2)$ which connects the two. Since the electroweak model dependence and the polar angle dependence of σ_α and $d\sigma_\alpha^{(\ell_1\ell_2)}$ are the same, we introduce a compact notation $\sigma_\alpha^{\{\ell_1\ell_2\}}$ where $\sigma_\alpha^{\{\ell_1\ell_2\}}$ stand for either σ_α or $\sigma_\alpha^{(\ell_1\ell_2)}$. Thus we write

$$
\begin{aligned}
\frac{d\sigma^{\{\ell_1\ell_2\}}}{d\cos\theta} &= \frac{3}{8}(1 + \cos^2\theta)\left(g_{11}\sigma_U^{1\,\{\ell_1\ell_2\}} + g_{12}\sigma_U^{2\,\{\ell_1\ell_2\}}\right) \\
&\quad + \frac{3}{4}\sin^2\theta\left(g_{11}\sigma_L^{1\,\{\ell_1\ell_2\}} + g_{12}\sigma_L^{2\,\{\ell_1\ell_2\}}\right) \\
&\quad + \frac{3}{4}\cos\theta\left(g_{43}\sigma_F^{3\,\{\ell_1\ell_2\}} + g_{44}\sigma_F^{4\,\{\ell_1\ell_2\}}\right).
\end{aligned}
\tag{5}
$$

The index $j = 1, 2, 3, 4$ in $\sigma_\alpha^{j\,\{\ell_1\ell_2\}}$ runs over the four linear combinations of bilinear products of vector and axial vector currents defined by

$$
\begin{aligned}
\sigma_\alpha^1 &= \frac{1}{2}(\sigma_\alpha^{VV} + \sigma_\alpha^{AA}), & \sigma_\alpha^2 &= \frac{1}{2}(\sigma_\alpha^{VV} - \sigma_\alpha^{AA}), \\
\sigma_\alpha^3 &= \frac{i}{2}(\sigma_\alpha^{VA} - \sigma_\alpha^{AV}), & \sigma_\alpha^4 &= \frac{1}{2}(\sigma_\alpha^{VA} + \sigma_\alpha^{AV}).
\end{aligned}
\tag{6}
$$

4

θ is the polar angle between the electron beam direction and the top quark direction.

The matrix g_{ij} $(i, j = 1, 2, 3, 4)$ specifies the electroweak model dependence of the $e^+ e^-$ cross section. For the present discussion we only need the components g_{11}, g_{12}, g_{43} and g_{44}. They are given by

$$
\begin{aligned}
g_{11} &= Q_f^2 - 2Q_f v_e v_f \operatorname{Re} \chi_Z + (v_e^2 + a_e^2)(v_f^2 + a_f^2)|\chi_Z|^2, \\
g_{12} &= Q_f^2 - 2Q_f v_e v_f \operatorname{Re} \chi_Z + (v_e^2 + a_e^2)(v_f^2 - a_f^2)|\chi_Z|^2, \\
g_{43} &= 2Q_f a_e a_f \operatorname{Im} \chi_Z, \\
g_{44} &= -2Q_f a_e a_f \operatorname{Re} \chi_Z + 4v_e a_e v_f a_f |\chi_Z|^2
\end{aligned}
\tag{7}
$$

where for the Standard Model $\chi_Z(q^2) = gM_Z^2 q^2/(q^2 - M_Z^2 + iM_Z\Gamma_Z)$ with M_Z and Γ_Z the mass and width of the Z^0 and $g = G_F(8\sqrt{2}\pi\alpha)^{-1} \approx 4.49 \times 10^{-5}\,\mathrm{GeV}^{-2}$. Q_f are the charges of the final state quarks to which the electroweak currents directly couple, v_e and a_e, v_f and a_f are the electroweak vector and axial vector coupling constants. For example, in the Weinberg–Salam model one has $v_e = -1 + 4\sin^2\theta_W$, $a_e = -1$ for leptons, $v_f = 1 - \frac{8}{3}\sin^2\theta_W$, $a_f = 1$ for up-type quarks $(Q_f = \frac{2}{3})$, and $v_f = -1 + \frac{4}{3}\sin^2\theta_W$, $a_f = -1$ for down-type quarks $(Q_f = -\frac{1}{3})$. At low energies, where only QED interactions survive, the only remaining components of the electroweak coupling matrix g_{ij} are $g_{11} = Q_f^2$ and $g_{12} = Q_f^2$. In this paper we use Standard Model couplings with $\sin^2\theta_W = 0.231$ and $M_Z = 91.188\,\mathrm{GeV}$, $\Gamma_Z = 2.487\,\mathrm{GeV}$ [26].

The hadronic building block is entirely determined by the hadron dynamics, i.e. by the current-induced production of a quark-antiquark pair which, in the $O(\alpha_s)$ case, is followed by gluon emission. At $O(\alpha_s)$ one also has to add the one-loop contribution. We shall work in terms of unpolarized and polarized hadron tensor components H_α^j and $H_\alpha^{j\,(\ell_1\ell_2)}$ where the spin decomposition is defined in complete analogy to Eq. (3). The notation closely follows the notation used of Ref. [14].

In the two-body case $e^+ e^- \to q(p_1)\bar{q}(p_2)$ (Born and one-loop contribution) the unpolarized rate components σ_α^j and the longitudinal spin-spin components $\sigma_\alpha^{j\,(\ell_1\ell_2)}$ are related to the corresponding two-body hadronic tensor components $H_\alpha^{j\,\{\ell_1\ell_2\}}$ via

$$
\sigma_\alpha^{j\,\{\ell_1\ell_2\}} = \frac{\pi\alpha^2 v}{3q^4} H_\alpha^{j\,\{\ell_1\ell_2\}}
\tag{8}
$$

where $v^2 = 1 - 4m_q^2/q^2 := 1 - \xi$. The helicity structure functions $H_\alpha^{j\,\{\ell_1\ell_2\}}$ $(\alpha = U, L, F)$ are obtained from the hadron tensor components $H_{\mu\nu}^{j\,\{\ell_1\ell_2\}}$ via covariant projection

$$
\begin{aligned}
H_U^{j\,\{\ell_1\ell_2\}} &= \left(-\hat{g}_{\mu\nu} - \frac{\hat{p}_1^\mu \hat{p}_1^\nu}{p_{1z}^2}\right) H_{\mu\nu}^{j\,\{\ell_1\ell_2\}}, \qquad
H_L^{j\,\{\ell_1\ell_2\}} = \frac{\hat{p}_1^\mu \hat{p}_1^\nu}{p_{1z}^2} H_{\mu\nu}^{\{\ell_1\ell_2\}}, \\
H_F^{j\,\{\ell_1\ell_2\}} &= i\varepsilon^{\mu\nu\alpha\beta} \frac{\hat{p}_{1\alpha} q_\beta}{p_{1z}\sqrt{q^2}} H_{\mu\nu}^{j\,\{\ell_1\ell_2\}}
\end{aligned}
\tag{9}
$$

where $\hat{g}_{\mu\nu} = g_{\mu\nu} - q_\mu q_\nu/q^2$ and $\hat{p}_{1\mu} = p_{1\mu} - (p_1 \cdot q)q_\mu/q^2$ are the four-transverse metric tensor and the four-transverse quark momentum, respectively. The two-body hadron tensor

$H_{\mu\nu}^{\{\ell_1\ell_2\}}$, finally, is defined by the product of matrix elements

$$H_{\mu\nu}^j(p_1, p_2, s_1^l, s_2^l) = \langle q(s_1^l)\bar{q}(s_2^l)|J_\mu^{V,A}|0\rangle\langle 0|J_\nu^{\dagger V,A}|q(s_1^l)\bar{q}(s_2^l)\rangle, \tag{10}$$

where, again, the index $j = 1, 2, 3, 4$ specifies the current composition in terms of the parity-even (for $j = 1, 2$) and parity-odd ($j = 3, 4$) products of the vector and the axial vector currents as defined in Eq. (6).

In the three-body case $e^+e^- \to q(p_1)\bar{q}(p_2)g(p_3)$ the hadron tensor $H_{\mu\nu}^j$ is obtained from the square of the current matrix elements according to

$$H_{\mu\nu}^j(p_1, p_2, p_3, s_1^l, s_2^l) = \sum_{\text{gluon spin}} \langle q(s_1^l)\bar{q}(s_2^l)g|J_\mu^{V,A}|0\rangle\langle 0|J_\nu^{\dagger V,A}|q(s_1^l)\bar{q}(s_2^l)g\rangle. \tag{11}$$

Note that the three-body hadron tensor in Eq. (11) has a mass dimension differing from that of the two-body hadron tensor in Eq. (10). The projection of the three-body hadron tensor onto the six helicity structure functions $H_\alpha^{\{\ell_1\ell_2\}}$ ($\alpha = U, L, F$) is done in identical fashion to the two-body case. What is finally needed is the relation between the differential rate components and the three-body helicity structure functions. The relation is given by

$$\frac{d\sigma_\alpha^{j\,\{\ell_1\ell_2\}}}{dy\,dz} = \frac{\pi\alpha^2 v}{3q^4}\left\{\frac{q^2}{16\pi^2 v}H_\alpha^{j\,\{\ell_1\ell_2\}}(y, z)\right\} \tag{12}$$

where we have explicitly referred to the phase space dependence of the three-body hadron tensor in order to set it aside from the two-body hadron tensor in Eq. (10). As kinematic variables we use the two energy-type variables $y = 1 - 2p_1q/q^2$ and $z = 1 - 2p_2q/q^2$.

We mention that the above formalism allows for a straightforward incorporation of transverse and longitudinal beam polarization effects [14]. For example, if one starts with longitudinally polarized beams, one has to effect the replacement

$$\begin{aligned}
g_{1i} &\to (1 - h^- h^+)g_{1i} + (h^- - h^+)g_{4i} & (i = 1, 2) \\
g_{4j} &\to (1 - h^- h^+)g_{4j} + (h^- - h^+)g_{1j} & (j = 3, 4)
\end{aligned} \tag{13}$$

where h^- and h^+ ($-1 \le h^\pm \le +1$) denote the longitudinal polarization of the electron and the positron beam, respectively. Clearly there is no interaction between the beams when $h^+ = h^- = \pm 1$. The additional electroweak components g_{41}, g_{42}, g_{13}, and g_{14} needed in Eqs. (13) are given by

$$\begin{aligned}
g_{41} &= 2Q_f a_e v_f \operatorname{Re}\chi_Z - 2v_e a_e(v_f^2 + a_f^2)|\chi_Z|^2, \\
g_{42} &= 2Q_f a_e v_f \operatorname{Re}\chi_Z - 2v_e a_e(v_f^2 - a_f^2)|\chi_Z|^2, \\
g_{13} &= -2Q_f v_e a_f \operatorname{Im}\chi_Z, \\
g_{14} &= 2Q_f v_e a_f \operatorname{Re}\chi_Z - 2(v_e^2 + a_e^2)v_f a_f|\chi_Z|^2.
\end{aligned} \tag{14}$$

The incorporation of transverse beam polarization is described in Ref. [14].

6

3 Born term contributions

Let us begin by listing the nonvanishing Born term contributions to the unpolarized and the polarized spin-spin two-body hadron tensor components. They can be obtained from the two-body hadron tensors in covariant fashion by using the projections (9) and the two-body representations of the spin vectors (25) and (26). An alternative and rather convenient approach is to use helicity amplitudes $h^{V,A}_{\lambda;\lambda_q\lambda_{\bar{q}}}$ in the c.m. frame where λ denotes the rest frame m-quantum number of the (γ^*, Z) (the quark momentum defines the z-direction). The helicity amplitudes are given by

$$
\begin{aligned}
h^V_{0;\pm\frac{1}{2}\pm\frac{1}{2}} &= -\sqrt{1-v^2}\,\sqrt{q^2}, & h^A_{0;\pm\frac{1}{2}\pm\frac{1}{2}} &= 0, \\
h^V_{\pm1;\pm\frac{1}{2}\mp\frac{1}{2}} &= -\sqrt{2}\sqrt{q^2}, & h^A_{\pm1;\pm\frac{1}{2}\mp\frac{1}{2}} &= \mp\sqrt{2}v\sqrt{q^2}.
\end{aligned}
\tag{15}
$$

One obtains

$$
\begin{aligned}
H^1_U(Born) &= 2N_c q^2(1+v^2), \\
H^2_U(Born) &= 2N_c q^2(1-v^2), \\
H^1_L(Born) &= H^2_L(Born) = N_c q^2(1-v^2), \\
H^4_F(Born) &= 4N_c q^2 v
\end{aligned}
\tag{16}
$$

and

$$
\begin{aligned}
H^{1\,(\ell_1\ell_2)}_U(Born) &= -2N_c q^2(1+v^2), \\
H^{2\,(\ell_1\ell_2)}_U(Born) &= -2N_c q^2(1-v^2), \\
H^{1\,(\ell_1\ell_2)}_L(Born) &= H^{2\,(\ell_1\ell_2)}_L(Born) = N_c q^2(1-v^2), \\
H^{4\,(\ell_1\ell_2)}_F(Born) &= -4N_c q^2 v.
\end{aligned}
\tag{17}
$$

For completeness we also list the single spin Born term contributions. They read

$$
\begin{aligned}
H^{3\,(\ell_{1,2})}_U &= 0, \\
H^{4\,(\ell_{1,2})}_U &= \pm 4N_C q^2 v, \\
H^{3\,(\ell_{1,2})}_L &= H^{4\,\ell_{1,2}}_L = 0, \\
H^{1\,(\ell_{1,2})}_F &= \pm 2N_C q^2(1+v^2), \\
H^{2\,(\ell_{1,2})}_F &= \pm 2N_C q^2(1-v^2),
\end{aligned}
\tag{18}
$$

where the upper and lower signs stand for the quark and antiquark case, respectively.[1] Note that one has the Born term relations

$$
\begin{aligned}
H^{1,2}_U(Born) &= -H^{1,2\,(\ell_1\ell_2)}_U(Born), \\
H^4_F(Born) &= -H^{4\,(\ell_1\ell_2)}_F(Born), \\
H^{1,2}_L(Born) &= H^{1,2\,(\ell_1\ell_2)}_L(Born).
\end{aligned}
\tag{19}
$$

---

[1]The signs of $H^{1,2\,\ell_2}_F$ differ from those in Ref. [27] because, contrary to [27], in the present paper we are always referring to the same polar angle in Eq. (5) for both the quark and antiquark case.

These relations can be seen to arise from angular momentum conservation at the Born term level where the produced quark and antiquark are in a back-to-back configuration. The easiest way to see this is by noting that at the Born level one has $H_{U,F}(\uparrow\uparrow) = H_{U,F}(\downarrow\downarrow) = 0$ and $H_L(\uparrow\downarrow) = H_L(\downarrow\uparrow) = 0$ from angular momentum conservation. The above Born term relations then follow from inserting the above zero entries into Eqs. (4) (with σ_α replaced by H_α). It is quite clear that the relations Eq. (19) no longer hold true at $O(\alpha_s)$ in general since the quark and antiquark are no longer back-to-back due to additional gluon emission.

Let us now introduce the normalized $\cos\theta$-dependent longitudinal spin-spin asymmetry $P^{\ell\ell}(\cos\theta)$ which is defined by

$$P^{\ell\ell}(\cos\theta) = \frac{\frac{3}{8}(1 + \cos^2\theta)\sigma_U^{(\ell_1\ell_2)} + \frac{3}{4}\sin^2\theta\ \sigma_L^{(\ell_1\ell_2)} + \frac{3}{4}\cos\theta\ \sigma_F^{(\ell_1\ell_2)}}{\frac{3}{8}(1 + \cos^2\theta)\sigma_U + \frac{3}{4}\sin^2\theta\ \sigma_L + \frac{3}{4}\cos\theta\ \sigma_F} \tag{20}$$

where, according to Eq. (5), the $\sigma_\alpha^{\{\ell_1\ell_2\}}$ are given by

$$\begin{aligned}
\sigma_\alpha^{\{\ell_1\ell_2\}} &= g_{11}\sigma_\alpha^{1\,\{\ell_1\ell_2\}} + g_{12}\sigma_\alpha^{2\,\{\ell_1\ell_2\}}, \qquad (\alpha = U, L) \\
\sigma_F^{\{\ell_1\ell_2\}} &= g_{43}\sigma_F^{3\,\{\ell_1\ell_2\}} + g_{44}\sigma_F^{4\,\{\ell_1\ell_2\}}.
\end{aligned} \tag{21}$$

As before the curly bracket notation $\{\ell_1\ell_2\}$ stands for either the unpolarized or the longitudinal spin-spin correlation case. Because $\sigma_\alpha^{j\,\{\ell_1\ell_2\}}$ and $H_\alpha^{j\,\{\ell_1\ell_2\}}$ are proportional to each other, one can freely substitute $H_\alpha^{j\,\{\ell_1\ell_2\}}$ for $\sigma_\alpha^{j\,\{\ell_1\ell_2\}}$ in Eq. (20).

In the forward and backward direction ($\cos\theta = \pm 1$) one finds the Born term relation

$$P^{\ell\ell}(Born; \cos\theta = \pm 1) = -1 \tag{22}$$

regardless of the energy $\sqrt{q^2}$ which follows again from angular momentum conservation since the spins of the quark and antiquark have to be aligned in the forward and backward direction. Formally this can be seen by substituting the Born term relations (19) into Eq. (20).

Next we discuss the limiting values of the longitudinal spin-spin correlation asymmetry at threshold $v \to 0$ and in the high energy limit $v \to 1$. At threshold $v = 0$ one finds[2]

$$\text{threshold:} \qquad P^{\ell\ell}(Born; \cos\theta) = -\cos^2\theta \tag{23}$$

which implies that the longitudinal spin-spin asymmetry vanishes at threshold at 90°, i.e. $P^{\ell\ell}(Born; \cos\theta = 0)_{\text{threshold}} = 0$. The angular average is $\langle P^{\ell\ell}(Born; \cos\theta)_{\text{threshold}} \rangle = -1/3$ in agreement with Ref. [6]. In the high energy limit $m_q/\sqrt{q^2} \to 0$ where the quark and antiquark spins become completely aligned, i.e. $\sigma_L = \sigma_L^{(\ell_1\ell_2)} = 0$, one has

$$\text{high energy limit:} \qquad P^{\ell\ell}(Born; \cos\theta) = -1 \tag{24}$$

independent of the polar orientation.

---

[2]Note that in the threshold region QCD binding effects modify the naive threshold results significantly.

8

4 $O(\alpha_s)$ tree graph contributions

The $O(\alpha_s)$ spin-dependent hadronic three-body tensor $H_{\mu\nu}(p_1, p_2, p_3, s_1^l, s_2^l)$ can easily be calculated from the relevant Feynman diagrams. In order to calculate the longitudinal spin-spin correlations one needs an explicit representation of the longitudinal spin components of the quark and antiquark. They are given by

$$(s_1^\ell)^\mu = \frac{s_1^\ell}{\sqrt{\xi}}(\sqrt{(1-y)^2 - \xi}; 0, 0, 1-y), \tag{25}$$

$$(s_2^\ell)^\mu = \frac{s_2^\ell}{\sqrt{\xi}}(\sqrt{(1-z)^2 - \xi}; (1-z)\sin\theta_{12}, 0, (1-z)\cos\theta_{12}) \tag{26}$$

where θ_{12} is the polar angle between the quark and the antiquark.[3] The polar angle is given by ($\xi = 4m_q^2/q^2 = 1 - v^2$, $y = 1 - 2p_1q/q^2$, $z = 1 - 2p_2q/q^2$)

$$\cos\theta_{12} = \frac{yz + y + z - 1 + \xi}{\sqrt{(1-y)^2 - \xi}\sqrt{(1-z)^2 - \xi}}. \tag{27}$$

In the two-body Born term case, where $y = z = 0$, one has $\cos\theta_{12} = -1$. The polarization four-vectors (25) and (26) then simplify to their expected two-body representations.

For the spin-spin dependent piece one obtains (with $N := \alpha_s N_c C_F q^2/4\pi v$, $R_y := \sqrt{(1-y)^2 - \xi}$ and $R_z := \sqrt{(1-z)^2 - \xi}$)

$$
\begin{aligned}
H_U^{1(\ell_1\ell_2)}(tree) =\ & \frac{N}{R_y^3 R_z}\Bigg[-2(2-\xi)(24 - 23\xi + \xi^2) \\
& +2(8-9\xi)(1-\xi)(2-\xi)\frac{1}{y} + 4(30 - 24\xi + 4\xi^2)y \\
& -2(44 - 26\xi + 3\xi^2)y^2 + 8(5-\xi)y^3 - 8y^4 \\
& +2\xi(2-\xi)(1-\xi)^2\left(\frac{1}{y^2} + \frac{1}{z^2}\right) - 6\xi(1-\xi)(2-\xi)\frac{y}{z^2} \\
& +4\xi(2-\xi)^2\frac{y^2}{z^2} - 4\xi(3-2\xi)\frac{y^3}{z^2} + 2\xi(2-\xi)\frac{y^4}{z^2} \\
& +2(16 - 11\xi)(1-\xi)(2-\xi)\frac{1}{z} - 4(1-\xi)^2(2-\xi)^2\frac{1}{yz} \\
& -2(2-\xi)(26 - 27\xi + 3\xi^2)\frac{y}{z} + 8(11 - 13\xi + 4\xi^2)\frac{y^2}{z} \\
& -4(1-\xi)(10-\xi)\frac{y^3}{z} + 8(1-\xi)\frac{y^4}{z}
\end{aligned}
$$

---

[3]In the three-body case the quark and antiquark are no longer back-to-back in general and thus the spins in the aligned spin configurations ($\uparrow\downarrow$) and ($\downarrow\uparrow$) are no longer parallel in general. However, in the $(t\bar{t})$-case the top and antitop quarks are quite "stiff" w.r.t. gluon radiation for the relevant lower energies. The average opening angle is $\langle\cos\theta_{12}\rangle = -0.996$ and $\langle\cos\theta_{12}\rangle = -0.980$ at $\sqrt{q^2} = 500\,\text{GeV}$ and $\sqrt{q^2} = 1000\,\text{GeV}$, respectively [28].

$$+8(5-3\xi)z - 2\xi(1-\xi)(2-\xi)\frac{z}{y^2}$$

$$-2(2-\xi)(6-9\xi+\xi^2)\frac{z}{y} - 4(6-3\xi+2\xi^2)yz$$

$$+8(1-2\xi)y^2z - 4(2-2\xi+\xi^2)z^2 + 2\xi(1-\xi)(2-\xi)\frac{z^2}{y^2}$$

$$+4(2-\xi)(1-2\xi)\frac{z^2}{y} + 8yz^2 - 16\xi yz^2 - 8y^2z^2\Big], \tag{28}$$

$$H_U^{2\,(\ell_1\ell_2)}(tree) = \frac{\xi N}{R_y^3 R_z}\Big[40 - 36\xi - 2\xi(1-\xi)^2\frac{1}{y^2} - 2(8-9\xi)(1-\xi)\frac{1}{y}$$

$$-2(12-\xi)y - 2(4-\xi)y^2 + 8y^3 - 2\xi(1-\xi)^2\frac{1}{z^2}$$

$$+6\xi(1-\xi)\frac{y}{z^2} - 2\xi(3-\xi)\frac{y^2}{z^2} + \frac{2\xi y^3}{z^2}$$

$$-2(16-11\xi)(1-\xi)\frac{1}{z} + 4(1-\xi)^2(2-\xi)\frac{1}{yz}$$

$$+2(24-23\xi+\xi^2)\frac{y}{z} - 2(16-5\xi)\frac{y^2}{z}$$

$$+2(4+\xi)\frac{y^3}{z} - 2(16-3\xi)z + 2\xi(1-\xi)\frac{z}{y^2}$$

$$+2(8-11\xi+\xi^2)\frac{z}{y} + 2(8-\xi)yz$$

$$+2(8-\xi)z^2 - 2\xi(1-\xi)\frac{z^2}{y^2} - 4(2-3\xi)\frac{z^2}{y} - 8yz^2\Big], \tag{29}$$

$$H_L^{1\,(\ell_1\ell_2)}(tree) = \frac{N}{R_y^3 R_z}\Big[-16 + 56\xi - 43\xi^2 + 5\xi^3 - \xi^2(1-\xi)^2\frac{1}{y^2}$$

$$-\xi(8-9\xi)(1-\xi)\frac{1}{y} + (32-70\xi+23\xi^2)y$$

$$-2(8-9\xi)y^2 - 6\xi y^3 + 2\xi y^4 - \xi^2(1-\xi)^2\frac{1}{z^2}$$

$$+3\xi^2(1-\xi)\frac{y}{z^2} - 2\xi^2(2-\xi)\frac{y^2}{z^2} + \frac{\xi^2 y^3}{z^2} - \frac{\xi^2 y^4}{z^2}$$

$$-\xi(16-11\xi)(1-\xi)\frac{1}{z} + 2\xi(1-\xi)^2(2-\xi)\frac{1}{yz}$$

$$+\xi(30-33\xi+5\xi^2)\frac{y}{z} - 9\xi(2-\xi)\frac{y^2}{z}$$

$$+\xi(2-\xi)\frac{y^3}{z} - \frac{2\xi y^4}{z} + (32-66\xi+23\xi^2)z$$

$$+\xi^2(1-\xi)\frac{z}{y^2} + \xi(10-15\xi+3\xi^2)\frac{z}{y} - (48-38\xi+\xi^2)yz$$

$$+2(8-\xi)y^2z + 4\xi y^3z - (16 - 26\xi + \xi^2)z^2 - \xi^2(1-\xi)\frac{z^2}{y^2}$$

$$-2\xi(3-4\xi)\frac{z^2}{y} + 2(8+\xi)yz^2 + 2\xi y^2z^2 \Bigg], \tag{30}$$

$$H_L^{2\,(\ell_1\ell_2)}(tree) = \frac{\xi N}{R_y^3 R_z}\Bigg[24 - 25\xi + 3\xi^2 - \xi(1-\xi)^2\frac{1}{y^2}$$

$$-(8-9\xi)(1-\xi)\frac{1}{y} - (22-9\xi)y + 2y^2 + 6y^3 - 2y^4$$

$$-\xi(1-\xi)^2\frac{1}{z^2} + 3\xi(1-\xi)\frac{y}{z^2} - \frac{2\xi y^2}{z^2} - \frac{\xi y^3}{z^2} + \frac{\xi y^4}{z^2}$$

$$-(16-11\xi)(1-\xi)\frac{1}{z} + 2(1-\xi)^2(2-\xi)\frac{1}{yz}$$

$$+(22-21\xi+\xi^2)\frac{y}{z} - (10-3\xi)\frac{y^2}{z} - (2-\xi)\frac{y^3}{z} + \frac{2y^4}{z}$$

$$-13(2-\xi)z + \xi(1-\xi)\frac{z}{y^2} + (10-15\xi+3\xi^2)\frac{z}{y}$$

$$+(18+\xi)yz + 2y^2z - 4y^3z + (10+\xi)z^2$$

$$-\xi(1-\xi)\frac{z^2}{y^2} - 2(3-4\xi)\frac{z^2}{y} - 2yz^2 - 2y^2z^2\Bigg], \tag{31}$$

$$H_F^{4\,(\ell_1\ell_2)}(tree) = \frac{2N}{R_y^2 R_z}\Bigg[-32 + 26\xi + \xi^2 + 2\xi(1-\xi)^2\frac{1}{y^2} + 16(1-\xi)^2\frac{1}{y}$$

$$+4(7-\xi)y - 4(4-\xi)y^2 + 4y^3 + 2\xi(1-\xi)^2\frac{1}{z^2}$$

$$-4\xi(1-\xi)\frac{y}{z^2} + \xi(4-3\xi)\frac{y^2}{z^2} - \xi(2-\xi)\frac{y^3}{z^2}$$

$$+6(4-3\xi)(1-\xi)\frac{1}{z} - 4(1-\xi)^2(2-\xi)\frac{1}{yz} - 4yz^2$$

$$-(28-32\xi+3\xi^2)\frac{y}{z} + 2(1-\xi)(8-\xi)\frac{y^2}{z} - 4(1-\xi)\frac{y^3}{z}$$

$$+2(4-\xi)(1+\xi)z - 2\xi(1-\xi)\frac{z}{y^2} - (12-16\xi+\xi^2)\frac{z}{y}$$

$$+4(1-\xi)yz - 4\xi z^2 + 2\xi(1-\xi)\frac{z^2}{y^2} + (4-6\xi-\xi^2)\frac{z^2}{y}\Bigg]. \tag{32}$$

The unpolarized helicity structure functions are needed for normalization purposes. They read (see e.g. Refs. [14])

$$H_U^1(tree) = \frac{N}{R_y^2}\Bigg[16 - 4\xi - 4\xi^2 - \frac{4\xi}{y^2} + \frac{6\xi^2}{y^2} - \frac{2\xi^3}{y^2} - \frac{16}{y} + \frac{32\xi}{y} - \frac{12\xi^2}{y}$$

$$-8\xi y - \frac{4\xi}{z^2} + \frac{6\xi^2}{z^2} - \frac{2\xi^3}{z^2} + \frac{8\xi y}{z^2} - \frac{4\xi^2 y}{z^2} - \frac{4\xi y^2}{z^2} - \frac{48}{z} + \frac{56\xi}{z}$$

11

$$
\begin{aligned}
& -\frac{16\xi^2}{z} + \frac{16}{yz} - \frac{32\xi}{yz} + \frac{20\xi^2}{yz} - \frac{4\xi^3}{yz} + \frac{56y}{z} - \frac{28\xi y}{z} - \frac{2\xi^2 y}{z} \\
& -\frac{32y^2}{z} + \frac{8y^3}{z} - 8\xi z + \frac{8z}{y} - \frac{4\xi z}{y} - \frac{2\xi^2 z}{y} + 8yz \Big], \tag{33}
\end{aligned}
$$

$$
\begin{aligned}
H_U^2(tree) \;=\; & \frac{\xi N}{R_y^2}\Big[8 + 2\xi - \frac{2\xi}{y^2} + \frac{2\xi^2}{y^2} - \frac{8}{y} + \frac{12\xi}{y} - \frac{2\xi}{z^2} + \frac{2\xi^2}{z^2} \\
& + \frac{4\xi y}{z^2} - \frac{2\xi y^2}{z^2} - \frac{24}{z} + \frac{16\xi}{z} + \frac{8}{yz} - \frac{12\xi}{yz} + \frac{4\xi^2}{yz} \\
& + \frac{24y}{z} - \frac{2\xi y}{z} - \frac{8y^2}{z} + 8z + \frac{2\xi z}{y} \Big], \tag{34}
\end{aligned}
$$

$$
\begin{aligned}
H_L^1(tree) \;=\; & \frac{N}{R_y^2}\Big[16 - 4\xi + \xi^2 - \frac{\xi^2}{y^2} + \frac{\xi^3}{y^2} - \frac{4\xi}{y} + \frac{6\xi^2}{y} - 16y + 4\xi y + 4\xi y^2 \\
& - \frac{\xi^2}{z^2} + \frac{\xi^3}{z^2} + \frac{2\xi^2 y}{z^2} + \frac{\xi^2 y^2}{z^2} - \frac{12\xi}{z} + \frac{8\xi^2}{z} + \frac{4\xi}{yz} - \frac{6\xi^2}{yz} + \frac{2\xi^3}{yz} \\
& + \frac{2\xi y}{z} + \frac{2\xi^2 y}{z} + \frac{2\xi y^3}{z} - 16z + 4\xi z - \frac{2\xi z}{y} + 2\xi yz \Big], \tag{35}
\end{aligned}
$$

$$
\begin{aligned}
H_L^2(tree) \;=\; & \frac{\xi N}{R_y^2}\Big[12\xi - \xi^2 - \frac{\xi^2}{y^2} + \frac{\xi^3}{y^2} - \frac{4\xi}{y} + \frac{6\xi^2}{y} - 4\xi y - 4\xi y^2 \\
& - \frac{\xi^2}{z^2} + \frac{\xi^3}{z^2} + \frac{2\xi^2 y}{z^2} - \frac{\xi^2 y^2}{z^2} - \frac{12\xi}{z} + \frac{8\xi^2}{z} + \frac{4\xi}{yz} - \frac{6\xi^2}{yz} + \frac{2\xi^3}{yz} \\
& + \frac{10\xi y}{z} - \frac{2\xi^2 y}{z} - \frac{2\xi y^3}{z} - 4\xi z - \frac{2\xi z}{y} - 2\xi yz \Big], \tag{36}
\end{aligned}
$$

$$
\begin{aligned}
H_F^4(tree) \;=\; & \frac{4N}{R_y}\Big[-\frac{\xi}{y^2} + \frac{\xi^2}{y^2} + -\frac{4}{y} + \frac{5\xi}{y} - \frac{\xi}{z^2} + \frac{\xi^2}{z^2} + \frac{\xi y}{z^2} - \frac{8}{z} + \frac{6\xi}{z} \\
& + \frac{4}{yz} - \frac{6\xi}{yz} + \frac{2\xi^2}{yz} + \frac{6y}{z} - \frac{2y^2}{z} + 2z + \frac{2z}{y} \Big]. \tag{37}
\end{aligned}
$$

5 One-loop contributions and $O(\alpha_s)$ corrections

The one-loop contributions to the unpolarized helicity structure functions can be taken from Refs. [13, 14]. Let us first list the contributions from the real part of the one-loop amplitude. For the unpolarized case one has

$$
\begin{aligned}
H_U^1(loop) \;&=\; 4N_c q^2 (\operatorname{Re} A + v^2 \operatorname{Re} C), \\
H_U^2(loop) \;&=\; 4N_c q^2 (\operatorname{Re} A - v^2 \operatorname{Re} C), \\
H_L^1(loop) \;&=\; H_L^2(loop) \;=\; 2N_c q^2 (\xi \operatorname{Re} A + v^2 \operatorname{Re} B), \\
H_F^4(loop) \;&=\; 4N_c q^2 v (\operatorname{Re} A + \operatorname{Re} C). \tag{38}
\end{aligned}
$$

For the longitudinal spin-spin correlation components one obtains

$$
\begin{aligned}
H_U^{1\,(\ell_1\ell_2)}(loop) &= -4N_c q^2 (\operatorname{Re} A + v^2 \operatorname{Re} C), \\
H_U^{2\,(\ell_1\ell_2)}(loop) &= -4N_c q^2 (\operatorname{Re} A - v^2 \operatorname{Re} C), \\
H_L^{1\,(\ell_1\ell_2)}(loop) &= H_L^{2\,(\ell_1\ell_2)}(loop) = 2N_c q^2 (\xi \operatorname{Re} A + v^2 \operatorname{Re} B), \\
H_F^{4\,(\ell_1\ell_2)}(loop) &= -4N_c q^2 v (\operatorname{Re} A + \operatorname{Re} C).
\end{aligned}
\tag{39}
$$

Since the one-loop contributions refer to two-body final states they also satisfy the two-body relations (19).

There are also contributions coming from the imaginary part of the vertex correction which multiplies the imaginary part of the Breit–Wigner function of the Z resonance as indicated in the electroweak model parameters g_{43} and g_{13} in Eqs. (7) and (14). The relevant hadron tensor component results from the V/A interference term in the F projection. Although these contributions are rather small (especially when one is far away from the Z resonance) they are included in our numerical results. The imaginary part contributions are given by

$$
\begin{aligned}
H_F^3(loop) &= -8N_c q^2 v \operatorname{Im} B, \\
H_F^{3\,(\ell_1\ell_2)}(loop) &= -8N_c q^2 v \operatorname{Im} B.
\end{aligned}
\tag{40}
$$

The one-loop form factors A, B, and C appearing in Eqs. (38) and (39) read ($C_F = 4/3$) [14]

$$
\begin{aligned}
\operatorname{Re} A &= -\frac{\alpha_s C_F}{4\pi} \Bigg[\left(2 + \frac{1+v^2}{v} \ln\left(\frac{1-v}{1+v}\right)\right) \ln\left(\frac{\Lambda q^2}{m^2}\right) + 3v \ln\left(\frac{1-v}{1+v}\right) + 4 \\
&\quad + \frac{1+v^2}{v} \left(\operatorname{Li}_2\left(\frac{2v}{1+v}\right) + \frac{1}{4}\ln^2\left(\frac{1-v}{1+v}\right) - \frac{\pi^2}{2}\right) \Bigg], \\
\operatorname{Re} B &= \frac{\alpha_s C_F}{4\pi} \frac{1-v^2}{v} \ln\left(\frac{1-v}{1+v}\right), \qquad \operatorname{Re} C = \operatorname{Re} A - 2\operatorname{Re} B, \\
\operatorname{Im} B &= \frac{\alpha_s C_F}{4\pi} \frac{1-v^2}{v} \pi.
\end{aligned}
\tag{41}
$$

The one-loop contributions have been infrared regularized by introducing a (small) gluon mass $m_g = \sqrt{\Lambda q^2}$ following Refs. [14].

What remains to be done is to perform the phase space integrations over the tree-graph contributions listed in Sec. 4. One first integrates over z and then over y. The relevant integration limits incorporating the auxiliary gluon mass are

$$
z_\pm(y) = \frac{2y}{4y+\xi} \left\{ 1 - y - \frac{1}{2}\xi + \Lambda + \frac{\Lambda}{y} \pm \frac{1}{y}\sqrt{(y-\Lambda)^2 - \Lambda\xi}\sqrt{(1-y)^2 - \xi} \right\}
\tag{42}
$$

and

$$
y_- = \sqrt{\Lambda\xi} + \Lambda, \qquad y_+ = 1 - \sqrt{\xi}.
\tag{43}
$$

13

The introduction of a (small) gluon mass distorts phase space away from the infrared singularity at $y = z = 0$. The infrared singularities in the tree graph and one-loop contributions cancel and one remains with finite remainders. It is quite clear that the finite result in the sum is independent of the specific regularization procedure. Finally, adding in the above one-loop contributions one obtains the $O(\alpha_s)$ corrections (loop + tree). For the sake of completeness we include in our results also the unpolarized hadron tensor components which are needed for the normalization of the longitudinal spin-spin asymmetry. One obtains

$$
\begin{aligned}
H_U^1(\alpha_s) &= N\Bigg[2(2+7\xi)v - 8(2-\xi)vt_{10} - 16(2-\xi)vt_{12} \\
&\quad +(48 - 48\xi + 7\xi^2)t_3 + 2\sqrt{\xi}(1 - \sqrt{\xi})(2 + 4\sqrt{\xi} - 3\xi)t_4 \\
&\quad -2\xi(2+3\xi)t_5 - 4(2-\xi)^2(t_8 - t_9)\Bigg],
\end{aligned} \tag{44}
$$

$$
\begin{aligned}
H_U^2(\alpha_s) &= \xi N\Bigg[12v - 8vt_{10} - 16vt_{12} + 2(6-\xi)t_3 + 2\sqrt{\xi}(1 - \sqrt{\xi})t_4 \\
&\quad +2\xi t_5 - 4(2-\xi)(t_8 - t_9)\Bigg],
\end{aligned} \tag{45}
$$

$$
\begin{aligned}
H_L^1(\alpha_s) &= N\Bigg[\left(8 - 23\xi + \frac{3\xi^2}{2}\right)v - 4\xi vt_{10} - 8\xi vt_{12} + \\
&\quad \xi\left(22 - 8\xi + \frac{3\xi^2}{4}\right)t_3 - 2\sqrt{\xi}(1 - \sqrt{\xi})(2 + 4\sqrt{\xi} - 3\xi)t_4 \\
&\quad +2\xi(2+3\xi)t_5 - 2\xi(2-\xi)(t_8 - t_9)\Bigg],
\end{aligned} \tag{46}
$$

$$
\begin{aligned}
H_L^2(\alpha_s) &= \xi N\Bigg[\frac{3}{2}(10-\xi)v - 4vt_{10} - 8vt_{12} + \left(6 - 4\xi - \frac{3\xi^2}{4}\right)t_3 \\
&\quad -2\sqrt{\xi}(1 - \sqrt{\xi})t_4 - 2\xi t_5 - 2(2-\xi)(t_8 - t_9)\Bigg],
\end{aligned} \tag{47}
$$

$$
\begin{aligned}
H_F^4(\alpha_s) &= N\Bigg[-16\sqrt{\xi}(1 - \sqrt{\xi}) - 16v^2(t_{10} + t_{11}) - 16(t_1 - t_2) \\
&\quad +8(2 - 3\xi)vt_3 - 4(4 - 5\xi)t_6 + 8(2 - \xi)v(t_7 - t_8)\Bigg]
\end{aligned} \tag{48}
$$

and

$$
\begin{aligned}
H_U^{1\,(\ell_1\ell_2)}(\alpha_s) &= N\Bigg[8 + 13\xi - \sqrt{\xi}(4 + 25\xi) - \frac{1}{2v}(10 - 7\xi - 19\xi^2) \\
&\quad -v\xi\left(t_1 + t_{12} - \frac{t_{11}}{2} - \ln 4\right) + \\
&\quad +2(2 - \xi)\left(\frac{2 - \xi}{2}(t_8 - t_{16}) + v(t_{10} + 2t_{12})\right)
\end{aligned}
$$

14

$$-\frac{1}{2}(8+2\xi+3\xi^2)t_{14}+\frac{1}{v^3}(8-15\xi+13\xi^2-4\xi^3)t_{15}$$

$$-\frac{1}{2v^2}(16-36\xi+55\xi^2-11\xi^3-4v^3\xi)t_{13}+$$

$$-\frac{1}{v^2}\left(4-3\xi+\xi^2+v^3(8-3\xi)\right)t_3\Bigg],\tag{49}$$

$$H_U^{2(\ell_1\ell_2)}(\alpha_s) = \xi N\Bigg[6-5\sqrt{\xi}-\frac{1}{v}-v\left(t_1+t_{12}-\frac{t_{11}}{2}-\ln 4\right)-\frac{1}{2}(8+\xi)t_{14}$$

$$+\frac{1}{2v^2}(4-\xi+4v^3)t_{13}+2\left(\frac{2-\xi}{2}(t_8-t_{16})+v(t_{10}+2t_{12})\right)$$

$$+\frac{1}{4v^3}(2-3\xi)(8-7\xi)t_{15}+\frac{1}{4v^2}\left(\xi(9-8\xi)-20v^3\right)t_3\Bigg],\tag{50}$$

$$H_L^{1(\ell_1\ell_2)}(\alpha_s) = N\Bigg[-\frac{3}{4}(24+22\xi-\xi^2)+\frac{1}{4}\sqrt{\xi}(48+112\xi+3\xi^2)$$

$$+\frac{1}{8v}(128-106\xi-81\xi^2+3\xi^3)+v\xi\left(t_1+t_{12}-\frac{t_{11}}{2}-\ln 4\right)$$

$$-\xi\left(\frac{2-\xi}{2}(t_8-t_{16})+v(t_{10}+2t_{12})\right)+\xi(6+\xi)t_{14}$$

$$-\frac{1}{8v^2}(64-32\xi-164\xi^2+51\xi^3-3\xi^4+16v^3\xi)t_{13}\tag{51}$$

$$-\frac{\xi}{4v^3}(28-24\xi+3\xi^2)t_{15}+\frac{\xi}{4v^2}(30-27\xi+4\xi^2+12v^3)t_3\Bigg],$$

$$H_L^{2(\ell_1\ell_2)}(\alpha_s) = \xi N\Bigg[\frac{1}{4}(34-3\xi)-\frac{3}{4}\sqrt{\xi}(12+\xi)-\frac{1}{8v}(46-65\xi+3\xi^2)$$

$$-(1+\xi)t_{14}+v\left(t_1+t_{12}-\frac{t_{11}}{2}-\ln 4\right)$$

$$-\left(\frac{2-\xi}{2}(t_8-t_{16})+v(t_{10}+2t_{12})\right)$$

$$+\frac{1}{8v^2}(80-136\xi+35\xi^2-3\xi^3-16v^3)t_{13}$$

$$-\frac{1}{2v^3}(4-9\xi+4\xi^2)t_{15}+\frac{1}{2v^2}(1-4\xi+2\xi^2+6v^3)t_3\Bigg],\tag{52}$$

$$H_F^{3(\ell_1\ell_2)}(\alpha_s) = N\Big[2\pi v\xi\Big],\tag{53}$$

$$H_F^{4(\ell_1\ell_2)}(\alpha_s) = N\Bigg[2\sqrt{\xi}+4v^2+\frac{2\xi}{v^2}(5-3\xi)(t_1-\ln 4)$$

$$+2v^2t_{11}-(4+\xi)t_{14}+2v(2-\xi)(t_8-t_{16}+t_{22})$$

$$+\frac{1}{4v^2}(16-32\xi+18\xi^2-\xi^3)t_{21}$$

15

$$+\frac{\xi}{v^3}(5 - 8\xi + 4\xi^2)(t_{20} - t_{19})$$

$$+\frac{\sqrt{\xi}}{2v^3}(8 - 11\xi + 3\xi^2 + 2\xi^3)(t_{20} + t_{19})$$

$$+\frac{\xi}{4v^2}(20 - 22\xi + \xi^2)(t_{18} - t_{17})$$

$$+\frac{\sqrt{\xi}}{4v^2}(16 - 10\xi - 5\xi^2)(t_{18} + t_{17})$$

$$-\frac{\sqrt{\xi}}{2v^2}(2 + 7\xi - 5\xi^2)(t_{12} - t_{10})$$

$$+\frac{1}{v^2}(2 - \xi)(1 + \xi)(t_{12} + t_{10})$$

$$+\frac{1}{v^3}(4 - 5\xi + 2\xi^3)t_{15} + \frac{1}{2v^2}(8 - 18\xi + \xi^2 + 5\xi^3)t_{13}$$

$$\left. -\frac{1}{4v^2}\left(8 - 18\xi + \xi^2 + 5\xi^3 + 2v(8 - 14\xi + 7\xi^2)\right)t_3 \right] \tag{54}$$

The unpolarized hadron tensor components $H_U^1(\alpha_s)$, $H_U^2(\alpha_s)$, $H_L^1(\alpha_s)$, $H_L^2(\alpha_s)$, and $H_F^4(\alpha_s)$ including the $O(\alpha_s)$ integrated rate functions t_i ($i = 1, 2, 3, 6, 7, 8, 9, 10, 12$) have been calculated and listed before in Ref. [14]. The integrated rate functions t_i ($i = 13, 14, 15, 16$) appear in the evaluation of the longitudinal spin-spin component $H_{U+L}^{4\,(\ell_1\ell_2)}$ and have been listed in Ref. [6]. In addition to the decay rate functions calculated in Ref. [6, 14] the spin-spin polar dependence contributions bring in a set of new decay rate functions t_i ($i = 17, 18, 19, 20, 21, 22$). The additional set of decay rate functions needed in the present application is given by

$$
\begin{aligned}
t_{17} =\ & \frac{5}{2}\ln\left(\frac{1+v}{2-\sqrt{\xi}}\right)\ln\left(\frac{2-\sqrt{\xi}}{2}\right) + \frac{1}{2}\ln\left(\frac{1-v}{2-\sqrt{\xi}}\right)\ln\left(\frac{1+v}{2}\right) \\
& + \mathrm{Li}_2(1) - \mathrm{Li}_2\left(\sqrt{\frac{1-v}{1+v}}\right) - 2\mathrm{Li}_2\left(\frac{\xi}{(2-\sqrt{\xi})^2}\right) \\
& + 2\mathrm{Li}_2\left(\frac{\sqrt{\xi}}{2-\sqrt{\xi}}\right) + \mathrm{Li}_2\left(\frac{(1-v)^2}{\sqrt{\xi}(2-\sqrt{\xi})}\right) - \mathrm{Li}_2\left(\frac{2-\sqrt{\xi}}{1+v}\right),
\end{aligned} \tag{55}
$$

$$
\begin{aligned}
t_{18} =\ & \ln\left(\frac{1+v}{2-\sqrt{\xi}}\right)\ln\left(\frac{2}{\sqrt{\xi}}\right) + \ln\left(\frac{\sqrt{\xi}(1+v)}{(2-\sqrt{\xi})^2}\right)\ln\left(\frac{2}{2+\sqrt{\xi}}\right) \\
& + \mathrm{Li}_2(-1) + \mathrm{Li}_2\left(\frac{2-\sqrt{\xi}}{2+\sqrt{\xi}}\right) - \mathrm{Li}_2\left(-\frac{2-\sqrt{\xi}}{2+\sqrt{\xi}}\right) \\
& - 2\mathrm{Li}_2\left(\frac{-\sqrt{\xi}}{2-\sqrt{\xi}}\right) + 2\mathrm{Li}_2\left(\frac{-\xi}{4-\xi}\right) - \mathrm{Li}_2\left(\frac{-(1-v)^2}{\sqrt{\xi}(2+\sqrt{\xi})}\right) \\
& - \mathrm{Li}_2\left(\frac{1+v}{2+\sqrt{\xi}}\right) + \mathrm{Li}_2\left(-\sqrt{\frac{1-v}{1+v}}\right),
\end{aligned} \tag{56}
$$

16

$$t_{19} = \ln\left(\frac{1+v}{1-v}\right)\ln\left(\frac{1+v}{2-\sqrt{\xi}}\right) + \ln^2\left(\frac{1+v}{2-\sqrt{\xi}}\right)$$
$$+ 2\text{Li}_2\left(\frac{1-v}{2-\sqrt{\xi}}\right) + 2\text{Li}_2\left(\frac{2-\sqrt{\xi}}{1+v}\right) - 4\text{Li}_2(1), \tag{57}$$

$$t_{20} = \ln\left(\frac{1+v}{1-v}\right)\ln\left(\frac{2-\sqrt{\xi}}{1+v}\right) + 2\text{Li}_2(-w) - 2\text{Li}_2(w)$$
$$- 2\text{Li}_2\left(-\frac{1-v}{2-\sqrt{\xi}}w\right) + 2\text{Li}_2\left(\frac{1+v}{2-\sqrt{\xi}}w\right), \tag{58}$$

$$t_{21} = 3\left(\frac{1}{2}\ln^2\left(\frac{1+v}{1-v}\right) + \ln\left(\frac{4}{\xi}\sqrt{\frac{1-v}{1+v}}\right)\ln\left(\frac{\sqrt{\xi}}{2-\sqrt{\xi}}\right)\right)$$
$$+ 3\left(\text{Li}_2\left(\frac{2-\sqrt{\xi}}{1+v}\right) - \text{Li}_2\left(\frac{2-\sqrt{\xi}}{1+v}\sqrt{\frac{1-v}{1+v}}\right)\right.$$
$$+ \text{Li}_2\left(\frac{1-v}{2-\sqrt{\xi}}\sqrt{\frac{1-v}{1+v}}\right) - \text{Li}_2\left(\frac{1-v}{2-\sqrt{\xi}}\right)\Bigg)$$
$$+ \text{Li}_2\left(\frac{4v}{(1+v)^2}\right) + \text{Li}_2\left(\frac{-2v}{1-v}\right) - \text{Li}_2\left(\frac{2v}{1+v}\right), \tag{59}$$

$$t_{22} = 2\ln\left(\frac{1+v}{2-\sqrt{\xi}}\right)\ln\left(\frac{2(1+\sqrt{\xi})(2-\sqrt{\xi})}{(1+v)^2}\right)$$
$$+ 4\text{Li}_2\left(\frac{\sqrt{\xi}-1+v}{2v}\right) - 4\text{Li}_2\left(\frac{(1-v)(\sqrt{\xi}-1+v)}{2v(2-\sqrt{\xi})}\right) \tag{60}$$

where

$$w = \sqrt{\frac{1+\sqrt{\xi}}{1-\sqrt{\xi}}}. \tag{61}$$

We have checked that the sum of $H_U^{1,2\,(\ell_1\ell_2)}(\alpha_s)$ and $H_L^{1,2\,(\ell_1\ell_2)}(\alpha_s)$ agrees with the form $H_{U+L}^{1,2\,(\ell_1\ell_2)}(\alpha_s)$ calculated in [6].

6   Massless QCD and the zero-mass limit of QCD

Before we turn to the numerical evaluation of the longitudinal spin-spin correlations, we would like to discuss the $m_q \to 0$ limit of our analytical results with the aim to compare them to the corresponding results obtained in massless QCD ($m_q = 0$). As is well-known by now, the $m_q \to 0$ limit in particular of the spin-flip contribution does not coincide with that of $m_q = 0$ QCD where there is no spin-flip [15, 16, 18, 13, 14].

The $m_q = 0$ expressions can be calculated in dimensional regularization as described in Ref. [14]. For the $O(\alpha_s)$ contributions one obtains

$$H_U^1(\alpha_s) = 4N_c q^2\frac{\alpha_s C_F}{4\pi}, \qquad H_U^{1\,(\ell_1\ell_2)}(\alpha_s) = -4N_c q^2\frac{\alpha_s C_F}{4\pi},$$

17

$$H_L^1(\alpha_s) \;=\; 8N_cq^2\frac{\alpha_sC_F}{4\pi}, \qquad H_L^{1\,(\ell_1\ell_2)}(\alpha_s) \;=\; -8N_cq^2\frac{\alpha_sC_F}{4\pi},$$
$$H_F^4(\alpha_s) \;=\; 0, \qquad H_F^{4\,(\ell_1\ell_2)}(\alpha_s) \;=\; 0. \tag{62}$$

The $O(\alpha_s)$ $m_q = 0$ single-spin functions $H_\alpha^{j\,(\ell_{1,2})}(\alpha_s)$ are given in Ref. [14] or can be read off from Eq. (66).

Let us now consider the $m_q \to 0$ limit of the integrated decay rate functions t_i discussed in Sec. 5. One obtains

$$t_1 \to \ln 4 - \frac{3}{2}\ln\left(\frac{4}{\xi}\right) \qquad t_2 \to \ln 4 - \frac{1}{2}\ln\left(\frac{4}{\xi}\right) \qquad t_3 \to \ln\left(\frac{4}{\xi}\right) \quad t_4 \to \frac{\pi^2}{2}$$

$$t_5 \to \frac{\pi^2}{6} - \frac{1}{4}\ln^2\left(\frac{4}{\xi}\right) \qquad t_6 \to \frac{\pi^2}{6} + \frac{1}{4}\ln^2\left(\frac{4}{\xi}\right) \qquad t_7 \to -\frac{\pi^2}{2} - \frac{1}{4}\ln^2\left(\frac{4}{\xi}\right)$$

$$t_8 \to -\frac{2\pi^2}{3} - \frac{1}{2}\ln^2\left(\frac{4}{\xi}\right) \qquad t_9 \to -\frac{2\pi^2}{3} - \frac{1}{2}\ln^2\left(\frac{4}{\xi}\right) \quad t_{10} \to \ln\left(\frac{4}{\xi}\right)$$

$$t_{11} \to \ln\left(\frac{4}{\xi}\right) \qquad\qquad t_{12} \to \ln\left(\frac{4}{\xi}\right) \qquad\qquad t_{13} \to 0$$

$$t_{14} \to \frac{\pi^2}{6} \qquad\qquad t_{15} \to \frac{\pi^2}{3} + \frac{1}{4}\ln^2\left(\frac{4}{\xi}\right) \qquad t_{16} \to -\frac{\pi^2}{6}$$

$$t_{17} \to 0 \qquad\qquad t_{18} \to 0 \qquad\qquad t_{19} \to -\frac{\pi^2}{3}$$

$$t_{20} \to -\frac{\pi^2}{6} \qquad\qquad t_{21} \to \frac{\pi^2}{3} + \frac{1}{4}\ln^2\left(\frac{4}{\xi}\right) \qquad t_{22} \to 0 \tag{63}$$

Using these limiting expressions one obtains for the $O(\alpha_s)$ $m_q \to 0$ unpolarized structure functions (loop + tree)

$$H_U^1(\alpha_s) = 4N_cq^2\frac{\alpha_sC_F}{4\pi}, \qquad H_L^1(\alpha_s) = 8N_cq^2\frac{\alpha_sC_F}{4\pi}, \qquad H_F^4(\alpha_s) = 0 \tag{64}$$

and, for the longitudinal spin-spin correlation functions,

$$H_U^{1(\ell_1,\ell_2)}(\alpha_s) \;=\; 12N_cq^2\frac{\alpha_sC_F}{4\pi} \;=\; (-4 + [16])N_cq^2\frac{\alpha_sC_F}{4\pi},$$
$$H_L^{1(\ell_1,\ell_2)}(\alpha_s) \;=\; -8N_cq^2\frac{\alpha_sC_F}{4\pi},$$
$$H_F^{4(\ell_1,\ell_2)}(\alpha_s) \;=\; 16N_cq^2\frac{\alpha_sC_F}{4\pi} \;=\; [16]N_cq^2\frac{\alpha_sC_F}{4\pi}. \tag{65}$$

With the square bracket notation we indicate the difference between the $O(\alpha_s)$ $m_q \to 0$ and $m_q = 0$ results which we call anomalous terms.[4] Note that the current-current structures for $j = 2, 3$ are zero in the limit $m_q \to 0$ (and also for $m_q = 0$).

---

[4]We use the phrase "anomalous flip contribution" since the same anomalous flip contribution contributes to the absorptive part of the VVA triangle diagram in the zero mass limit of QCD which in turn can be related to the well-known axial anomaly via a dispersion relation approach [29].

For completeness we also list the $O(\alpha_s)$ $m_q \to 0$ single-spin functions using the same square bracket notation. They read [14]

$$
\begin{aligned}
H_U^{4\,(\ell_{1,2})}(\alpha_s) &= \pm(4 - [8])N_c q^2 \frac{\alpha_s C_F}{4\pi}, \\
H_L^{4\,(\ell_{1,2})}(\alpha_s) &= \pm(8 - [0])N_c q^2 \frac{\alpha_s C_F}{4\pi}, \\
H_F^{1\,(\ell_{1,2})}(\alpha_s) &= \pm(0 - [8])N_c q^2 \frac{\alpha_s C_F}{4\pi}.
\end{aligned}
\tag{66}
$$

We finally collect all our $m_q \to 0$ results, including the Born term contributions Eqs. (16) and (17), where we make use of the representation Eq. (3). Again we split off the anomalous contributions using the square bracket notation. One obtains ($C_F = 4/3$ is made explicit here)

$$
\begin{aligned}
H_U^1(s_1^\ell, s_2^\ell) &= \frac{1}{4}\Big(H_U^1 + H_U^{1\,(\ell_1 \ell_2)} s_1^\ell s_2^\ell\Big) \\
&= N_c q^2 \left((1 - s_1^\ell s_2^\ell)\left(1 + \frac{1}{3} \times \frac{\alpha_s}{\pi}\right) + \left[\frac{4}{3} \times \frac{\alpha_s}{\pi} s_1^\ell s_2^\ell\right]\right), \\
H_L^1(s_1^\ell, s_2^\ell) &= \frac{1}{4}\Big(H_L^1 + H_L^{1\,(\ell_1 \ell_2)} s_1^\ell s_2^\ell\Big) \\
&= N_c q^2 (1 - s_1^\ell s_2^\ell)\left(0 + \frac{2}{3} \times \frac{\alpha_s}{\pi} + [0]\right), \\
H_F^1(s_1^\ell, s_2^\ell) &= \frac{1}{4}\Big(H_F^{1\,(\ell_1)} s_1^\ell + H_F^{1\,(\ell_2)} s_2^\ell\Big) \\
&= N_c q^2 (s_1^\ell - s_2^\ell)\left(1 + 0 \times \frac{\alpha_s}{\pi} - \left[\frac{2}{3} \times \frac{\alpha_s}{\pi}\right]\right), \\
H_U^4(s_1^\ell, s_2^\ell) &= \frac{1}{4}\Big(H_U^{4\,(\ell_1)} s_1^\ell + H_U^{4\,(\ell_2)} s_2^\ell\Big) \\
&= N_c q^2 (s_1^\ell - s_2^\ell)\left(1 + \frac{1}{3} \times \frac{\alpha_s}{\pi} - \left[\frac{2}{3} \times \frac{\alpha_s}{\pi}\right]\right), \\
H_L^4(s_1^\ell, s_2^\ell) &= \frac{1}{4}\Big(H_L^{4\,(\ell_1)} s_1^\ell + H_L^{4\,(\ell_2)} s_2^\ell\Big) \\
&= N_c q^2 (s_1^\ell - s_2^\ell)\left(0 + \frac{2}{3} \times \frac{\alpha_s}{\pi} + [0]\right), \\
H_F^4(s_1^\ell, s_2^\ell) &= \frac{1}{4}\Big(H_F^4 + H_F^{4\,(\ell_1 \ell_2)} s_1^\ell s_2^\ell\Big) \\
&= N_c q^2 \left((1 - s_1^\ell s_2^\ell)\left(1 + 0 \times \frac{\alpha_s}{\pi}\right) + \left[\frac{4}{3} \times \frac{\alpha_s}{\pi} s_1^\ell s_2^\ell\right]\right).
\end{aligned}
\tag{67}
$$

In Tables 1 and 2 we list all $m_q = 0$ and $m_q \to 0$ contributions to the various spin configurations for the parity-even (VV) and parity-odd (VA) current contributions using the representation Eq. (67). We have again used the square bracket notation to denote the anomalous contributions. The nonvanishing anomalous spin-flip contribution proportional to [4/3] in Table 1 e.g. in the ($\uparrow\uparrow$) spin configuration agrees with the corresponding result in [16] where this contribution was referred to as the chirality breaking contribution.

19

VV	U	L	F
$(\uparrow\uparrow)$	$0 + \dfrac{\alpha_s}{\pi}\left(0 + \left[\dfrac{4}{3}\right]\right)$	$0 + \dfrac{\alpha_s}{\pi}\left(0 + [0]\right)$	$0 + \dfrac{\alpha_s}{\pi}\left(0 + [0]\right)$
$(\uparrow\downarrow)$	$2 + \dfrac{\alpha_s}{\pi}\left(\dfrac{2}{3} - \left[\dfrac{4}{3}\right]\right)$	$0 + \dfrac{\alpha_s}{\pi}\left(\dfrac{4}{3} + [0]\right)$	$2 + \dfrac{\alpha_s}{\pi}\left(0 - \left[\dfrac{4}{3}\right]\right)$
$(\downarrow\uparrow)$	$2 + \dfrac{\alpha_s}{\pi}\left(\dfrac{2}{3} - \left[\dfrac{4}{3}\right]\right)$	$0 + \dfrac{\alpha_s}{\pi}\left(\dfrac{4}{3} + [0]\right)$	$-2 + \dfrac{\alpha_s}{\pi}\left(0 + \left[\dfrac{4}{3}\right]\right)$
$(\downarrow\downarrow)$	$0 + \dfrac{\alpha_s}{\pi}\left(0 + \left[\dfrac{4}{3}\right]\right)$	$0 + \dfrac{\alpha_s}{\pi}\left(0 + [0]\right)$	$0 + \dfrac{\alpha_s}{\pi}\left(0 + [0]\right)$

Table 1: Born term and $O(\alpha_s)$ corrections to specific spin configurations (first column) in $\mathrm{QCD}(m_q = 0)$ and $\mathrm{QCD}(m_q \to 0)$ for the parity-even current contributions. The entries are given in terms of contributions to the hadron tensor components $H_\alpha^{VV}(s_1^\ell, s_2^\ell) = H_U^{AA}(s_1^\ell, s_2^\ell)$ $(\alpha = U, L, F)$ in units of $N_c q^2$. Anomalous contributions are shown in square brackets.

Using the $m_q \to 0$ limiting expressions Eqs. (64) and (65) one finally obtains for the longitudinal spin-spin asymmetry

$$
\begin{aligned}
P^{\ell\ell}(\cos\theta) &= -1 + [4]\frac{\alpha_s C_F}{4\pi}\left(1 + \left(\frac{(1 + \cos^2\theta + 4\sin^2\theta)g_{11}}{(1 + \cos^2\theta)g_{11} + 2\cos\theta\, g_{44}}\right)\frac{\alpha_s C_F}{4\pi}\right)^{-1} \\
&= -1 + [4]\frac{\alpha_s C_F}{4\pi} + O(\alpha_s^2).
\end{aligned}
\tag{68}
$$

where we again have encased the "4" in square brackets in order to identify the contribution as anomalous. The result in Eq. (68) is independent of the flavour of the quark and thereby also holds for polarized lepton pair production $e^+e^- \to \mu^+\mu^-, \tau^+\tau^-$ replacing, of course, $C_F\alpha_s$ by α. We emphasize again that the normal $m_q = 0$ contributions lead to the value $P^{\ell\ell}(\cos\theta) = -1$ in the high energy limit. It is quite remarkable that the anomalous contributions do not show any $\cos\theta$ dependence at order $O(\alpha_s)$.

7 Anomalous contributions from the universal splitting function

It was shown e.g. in Ref. [18] that, in the limit $m_e \to 0$, there is a finite helicity flip radiation (i.e. $e_L \to e_R + \gamma$ and $e_R \to e_L + \gamma$) which arises from collinear photon emission. It can be described in terms of a universal splitting function $D_{hf}^{\mathrm{anom}} = \frac{\alpha}{2\pi}z$ where z is the fractional energy of the photon (not to be confused with the energy-type variable used in this paper). In this order of perturbation theory the derivation of Ref. [18] can be directly transscribed to the QCD case where one now has

$$
D_{hf}^{\mathrm{anom}} = C_F \frac{\alpha_s}{2\pi} z.
\tag{69}
$$

VA	U	L	F
$(\uparrow\uparrow)$	$0 + \dfrac{\alpha_s}{\pi}\left(0 + [0]\right)$	$0 + \dfrac{\alpha_s}{\pi}\left(0 + [0]\right)$	$0 + \dfrac{\alpha_s}{\pi}\left(0 + \left[\dfrac{4}{3}\right]\right)$
$(\uparrow\downarrow)$	$2 + \dfrac{\alpha_s}{\pi}\left(\dfrac{2}{3} - \left[\dfrac{4}{3}\right]\right)$	$0 + \dfrac{\alpha_s}{\pi}\left(\dfrac{4}{3} + [0]\right)$	$2 + \dfrac{\alpha_s}{\pi}\left(0 - \left[\dfrac{4}{3}\right]\right)$
$(\downarrow\uparrow)$	$-2 + \dfrac{\alpha_s}{\pi}\left(-\dfrac{2}{3} + \left[\dfrac{4}{3}\right]\right)$	$0 + \dfrac{\alpha_s}{\pi}\left(-\dfrac{4}{3} + [0]\right)$	$2 + \dfrac{\alpha_s}{\pi}\left(0 - \left[\dfrac{4}{3}\right]\right)$
$(\downarrow\downarrow)$	$0 + \dfrac{\alpha_s}{\pi}\left(0 + [0]\right)$	$0 + \dfrac{\alpha_s}{\pi}\left(0 + [0]\right)$	$0 + \dfrac{\alpha_s}{\pi}\left(0 + \left[\dfrac{4}{3}\right]\right)$

Table 2: Born term and $O(\alpha_s)$ corrections to specific spin configurations (first column) in QCD($m_q = 0$) and QCD($m_q \to 0$) for the parity-odd current contributions. The entries are given in terms of contributions to the hadron tensor components $H_U^{VA}(s_1^\ell, s_2^\ell) = H_U^{AV}(s_1^\ell, s_2^\ell)$, $H_L^{VA}(s_1^\ell, s_2^\ell) = H_L^{AV}(s_1^\ell, s_2^\ell)$, and $H_F^{VA}(s_1^\ell, s_2^\ell) = H_F^{AV}(s_1^\ell, s_2^\ell)$ in units of $N_c q^2$. Anomalous contributions are shown in square brackets.

Integrating over the fractional energy z gives

$$H_{hf}^{\text{anom}} = \int_0^1 H(Born) C_F \frac{\alpha_s}{2\pi} z \, dz = C_F \frac{\alpha_s}{4\pi} H(Born) \tag{70}$$

where we have, for the sake of simplicity, dropped all indices on the hadron tensor $H(Born)$.

One knows that there is no anomalous contribution to a given fermion transition when one integrates over the whole two-body phase space and one sums over the two spin states of a given final fermion. This was explicitly demonstrated for muon decay $\mu^- \to e^- \bar{\nu}_e \nu_\mu$ in Ref. [19] where the $O(\alpha)$ contributions to the two final electron spin states $e_L \to e_R + \gamma$ and $e_L \to e_L + \gamma$ were calculated in the limit $m_e \to 0$. There was an anomalous spin-flip contribution to $e_L \to e_R + \gamma$ determined by the universal splitting function in Eq. (69) accompanied by an anomalous non-flip contribution to $e_L \to e_L + \gamma$ of equal and opposite strength. When summing the spin-flip and non-flip contributions the anomalous terms cancelled leading to a "normal" unpolarized rate. This implies that, when integrating over the whole phase space, every anomalous spin-flip contribution is accompanied by an anomalous non-flip contribution of equal and opposite strength. As shown e.g. in Ref. [18] the photon in the collinear emission process $e_L \to e_R + \gamma$ is lefthanded, i.e. one has $e_L \to e_R + \gamma_L$ in agreement with angular momentum conservation. By the same token the anomalous non-flip contribution must vanish in the forward direction as has been explicitly demonstrated in [18].

The same empirical pattern is observed in the $m_q \to 0$ limit of $e^+ e^- \to q\bar{q}g$. Consider, for example, gluon emission from the quark and keep the antiquark helicity fixed at $\bar{q}_L$. The anomalous spin-flip contribution $q_L \to q_R + g$ is determined by the universal splitting function Eq. (69) which is cancelled by the residual non-flip contribution $q_L \to q_L + g$ when one takes the sum of the two, i.e. the sum has no residual mass effects. We have verified by

explicit calculation that the residual non-flip contribution originates from the near-forward region irrespective of the fact that the non-flip contribution vanishes in the exact forward direction.

In this way one can determine the anomalous flip and non-flip contributions to each spin configuration. In fact, one reproduces the anomalous entries in Table 1 and Table 2 by using the relations

$$
\begin{aligned}
[\uparrow\uparrow] &= (\uparrow\downarrow_{[hf]}) + (\downarrow_{[hf]}\uparrow) \\
&= \left((\uparrow\downarrow)_{Born} + (\downarrow\uparrow)_{Born}\right)\left[C_F\frac{\alpha_s}{4\pi}\right]
\end{aligned}
\tag{71}
$$

and

$$
\begin{aligned}
[\uparrow\downarrow] &= (\uparrow\downarrow_{[nf]}) + (\uparrow_{[nf]}\downarrow) \\
&= -2(\uparrow\downarrow)_{Born}\left[C_F\frac{\alpha_s}{4\pi}\right],
\end{aligned}
\tag{72}
$$

and correspondingly for the spin configurations $[\downarrow\uparrow]$ and $[\downarrow\downarrow]$. The anomalous contributions to the spin-spin structure function $H_U^{\ell_1\ell_2}$ can be seen to be 50% flip and 50% non-flip. The anomalous contribution to the single-spin structure function $H_U^{\ell_1}$ derives entirely from the anomalous non-flip contribution contrary to what was stated in [14]. This, in particular, means that the universal anomalous spin-flip contribution will not show up in single-spin polarization measurements, but contributes at the 50% level to spin-spin polarization measurements.

One can explicitly verify from the entries of Table 1 and Table 2 that the anomalous flip and non-flip contributions to a given quark or antiquark transition cancel upon summation. We mention that the "normal" $O(\alpha_s)$ $m_q = 0$ contributions in Table 1 and Table 2 can be determined from Eq. (67).

8 Numerical results

We are now in the position to discuss our numerical results for the $\cos\theta$-dependent normalized longitudinal spin-spin asymmetry $P^{\ell\ell}(\cos\theta)$ defined in Eq. (20).

In Fig. 1 we show the $\cos\theta$ dependence of the $O(\alpha_s)$ longitudinal spin-spin correlation function $P^{\ell\ell}(\cos\theta)$ in $e^+e^- \to t\bar{t}$ for the four different center-of-mass energies $\sqrt{q^2} = 360$, 400, 500, and 1000 GeV. At $\sqrt{q^2} = 360$ GeV one is sufficiently far above the $(t\bar{t})$-threshold for perturbative QCD to apply. The above range of center-of-mass energies is the envisaged range for the proposed linear colliders. At the lowest shown energy $\sqrt{q^2} = 360$ GeV the $\cos\theta$ distribution of $P^{\ell\ell}$ is still quite close to the threshold Born term distribution $P^{\ell\ell}(\cos\theta) = -\cos^2\theta$ (see Eq. (23)). However, one already notes a small forward-backward asymmetric effect which is induced by the (VA)-interference term $H_F^{4\{\ell_1\ell_2\}}$. In the forward and backward directions $\cos\theta = \pm 1$ the longitudinal spins are quite close to being 100% aligned as is true for the Born term case (see Eq. (22)). Away from the forward and backward direction the destructive longitudinal contribution $H_L^{j\,(\ell_1\ell_2)}$ $(j = 1, 2)$ comes into play
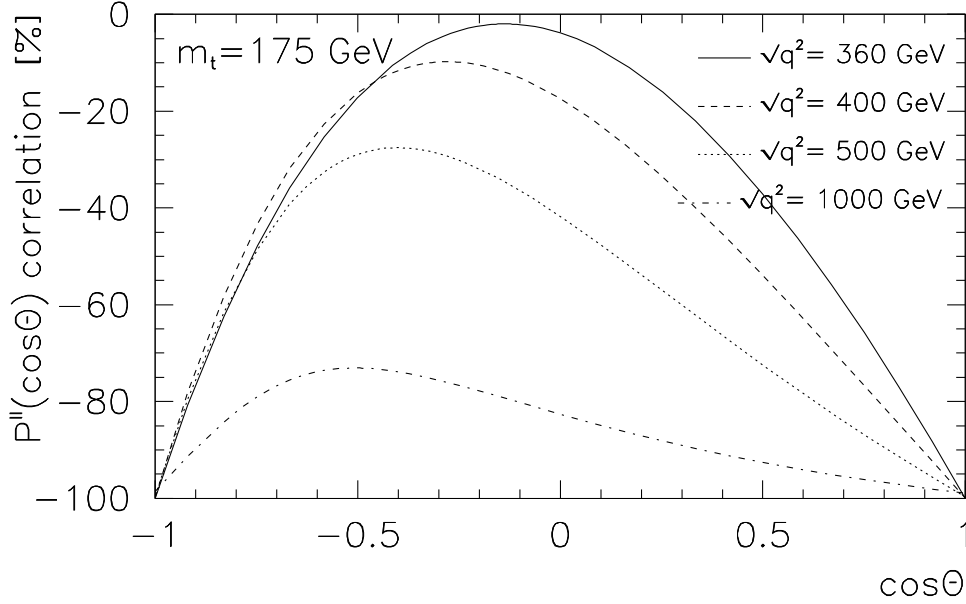
Figure 1: $O(\alpha_s)$ polar angle dependence of the longitudinal spin-spin correlation asymmetry in $e^+e^- \to t\bar{t}$ at $\sqrt{q^2} = 360$, 400, 500, and 1000 GeV. We always take $m_t = 175$ GeV as default value.

and reduces $P^{\ell\ell}(\cos\theta)$ from the maximal $m_q = 0$ value $P^{\ell\ell} \simeq -1$. As the energy is increased, $H_L^{j\,(\ell_1\ell_2)}$ becomes smaller and thus $P^{\ell\ell}(\cos\theta)$ becomes flatter. At $\sqrt{q^2} = 1000$ GeV the alignment of the spins of the top and antitop exceeds $\simeq 75\%$ over most of the range of $\cos\theta$.

In Fig. 2 we exhibit the relative size of the $O(\alpha_s)$ corrections which we define by the measure

$$\Delta P^{\ell\ell}(\cos\theta) = \frac{P^{\ell\ell}(\cos\theta)|_{O(\alpha_s)} - P^{\ell\ell}(\cos\theta)|_{Born}}{P^{\ell\ell}(\cos\theta)|_{Born}}. \tag{73}$$

Fig. 2 shows that the $O(\alpha_s)$ corrections to $P^{\ell\ell}(\cos\theta)$ are strongly polar angle dependent. They are not very small and can reach values as high as $\simeq 4\%$. It is quite remarkable that the radiative corrections for the lowest energy $\sqrt{q^2} = 360$ GeV are very close to zero in the forward and backward directions. As the energy is increasing the radiative corrections in the forward and backward directions become larger and they start approaching their anomalous limiting value Eq. (68).

In Fig. 2 we have also included a plot of $\Delta P^{\ell\ell}(\cos\theta)$ for the rather large center-of-mass energy of $\sqrt{q^2} = 10^4$ GeV (we are not implying that such center-of-mass energies will ever be reached in terrestrial laboratories). The purpose is to exhibit the anomalous contributions induced by the $O(\alpha_s)$ corrections when $m_q/\sqrt{q^2} \to 0$. In terms of the measure $\Delta P^{\ell\ell}(\cos\theta)$ defined in Eq. (73) one has in the high energy limit (see Eq.(68))

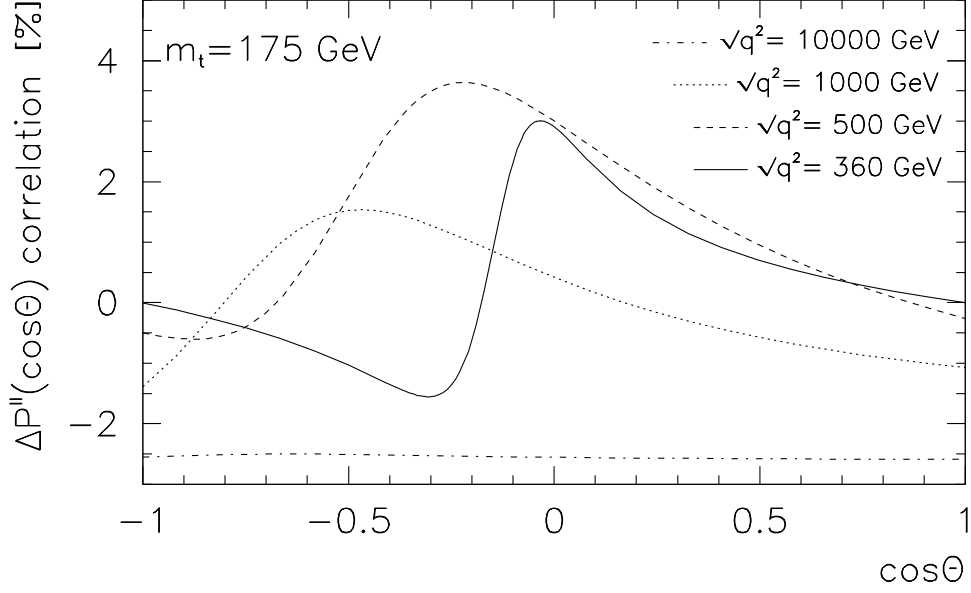$$\Delta P^{\ell\ell}(\cos\theta) = -[4]\frac{\alpha_s}{3\pi}. \tag{74}$$

23

Figure 2: Relative size of $O(\alpha_s)$ corrections to the longitudinal spin-spin correlation asymmetry in $e^+e^- \to t\bar{t}$ at $\sqrt{q^2} = 360, 500, 1000,$ and $10000\,\mathrm{GeV}$

.

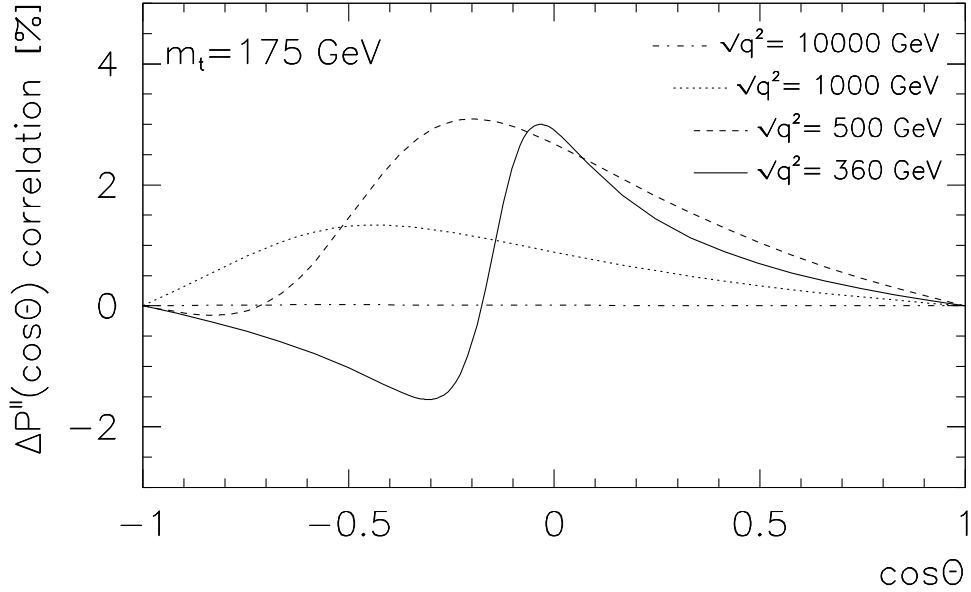Figure 3: Relative size of $O(\alpha_s)$ corrections to the longitudinal spin-spin correlation asymmetry in $e^+e^- \to t\bar{t}$ in the soft gluon approximation at $\sqrt{q^2} = 360, 500, 1000,$ and $10000\,\mathrm{GeV}$

.

Using $\alpha_s(\sqrt{q^2} = 10^4\,\text{GeV}) = 0.0712$ one numerically has $\Delta P^{\ell\ell}(\cos\theta) = -0.0303$ which is quite close to the value $\simeq -0.026$ shown in Fig. 2. The remaining difference can be traced to non-asymptotic effects.

In order to highlight the importance of hard gluon emission for the radiatively corrected longitudinal spin-spin asymmetry we have determined $\Delta P^{\ell\ell}(\cos\theta)$ in the soft gluon approximation as has also been employed in Ref. [3]. Fig. 3 shows a plot of $\Delta P^{\ell\ell}(\cos\theta)$ in the soft gluon approximation with the gluon energy integrated to its maximal energy. Since the soft gluon approximation is essentially a two-body approximation the radiative corrections can be seen to vanish in the forward and backward directions as discussed in Sec. 3. For the lowest energy $\sqrt{q^2} = 360\,\text{GeV}$ the corresponding two curves in Figs. 2 and 3 practically lie on top of each other since there there is very little phase space left for gluon emission. At $\sqrt{q^2} = 500\,\text{GeV}$ the difference between the full and approximate calculations becomes noticeable. In particular the $\cos\theta$-dependence of the full calculation is more pronounced. The same holds true for $\sqrt{q^2} = 1000\,\text{GeV}$ where the difference between the full and approximate calculation becomes as large as $\approx 1\%$ in the forward and backward directions. At $\sqrt{q^2} = 10000\,\text{GeV}$ one has $\Delta P^{\ell\ell}(\cos\theta) \approx 0$ in the the soft gluon approximation as expected whereas $\Delta P^{\ell\ell}(\cos\theta) \approx -2.6\%$ in the full calculation due to the anomalous contributions as discussed before.

The relatively small value of the $O(\alpha_s)$ correction for the longitudinal spin-spin asymmetry in Fig. 2 has to be contrasted with the large $O(\alpha_s)$ corrections to the cross section as shown in Fig. 4. For example, at $\sqrt{q^2} = 500\,\text{GeV}$ the $O(\alpha_s)$ corrections to the cross section amount to 15.4%. The reason that the radiative corrections to $P^{\ell\ell}$ are smaller than those for the rate is that the $O(\alpha_s)$ corrections in the numerator and denominator of $P^{\ell\ell}$ tend to go in the same direction and thus tend to cancel when one takes the ratio. However, this is not true for the anomalous contribution which contributes only to the numerator.

It is quite remarkable that the radiative corrections to $P^{\ell\ell}$ in the forward and backward directions are not small for the higher energies even if they only arise from non-Born-term-like hard gluon emission. Compare this to the corresponding case of top quark decay $t \to b + W_R^+$ where the right-handed W_R^+ is again only populated by non-Born-term-like hard gluon emission. In the case the radiative corrections amount to only 0.1% of the total Born term rate [30]. The explanation is that in the $e^+e^- \to t\bar{t}$ case one is sensitive to the enhanced forward hard gluon emission region whereas in the $t \to b + W_R^+$ case there is no such enhancement.

In Fig. 5 we display the polar angle dependence of the $O(\alpha_s)$ differential cross section for $(t\bar{t})$-production in e^+e^--annihilation. As Fig. 5 shows, the cross section strongly peaks in the forward direction. For example, for $\sqrt{q^2} = 1000\,\text{GeV}$ there is more than a factor of 10 cross section difference between the forward and backward directions. The fact that the cross sections peak so strongly in the forward direction is quite welcome from the point of view of checking the $O(\alpha_s)$ prediction for the longitudinal spin-spin asymmetry which, as remarked on before, is close to its $m_q = 0$ value $P^{\ell\ell} = -100\%$ in the forward direction.

In Figs. 6–8 we show the corresponding plots for $(b\bar{b})$-production at center-of-mass energies of $\sqrt{q^2} = 10$, 20 and 50 GeV and at the Z pole $(m_Z = 91.188\,\text{GeV})$. We use a pole mass of $m_b = 4.8\,\text{GeV}$ for the bottom quark. In Fig. 6 we show the polar angle dependence
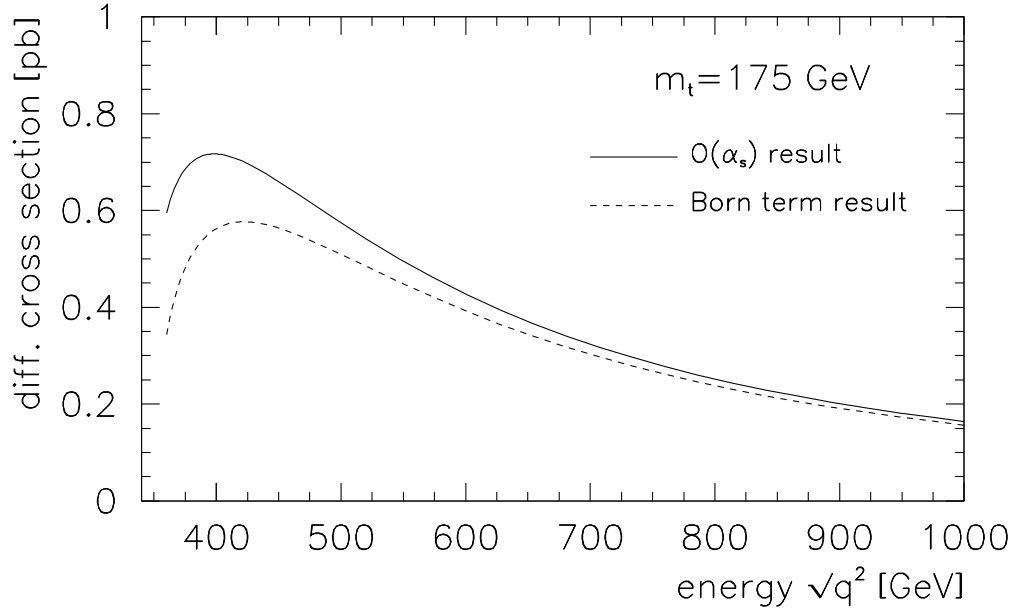
Figure 4: Differential cross section for $e^+e^- \to t\bar{t}$ at different center-of-mass energies $\sqrt{q^2}$. Shown are Born term results (dashed line) and $O(\alpha_s)$ results (solid line)
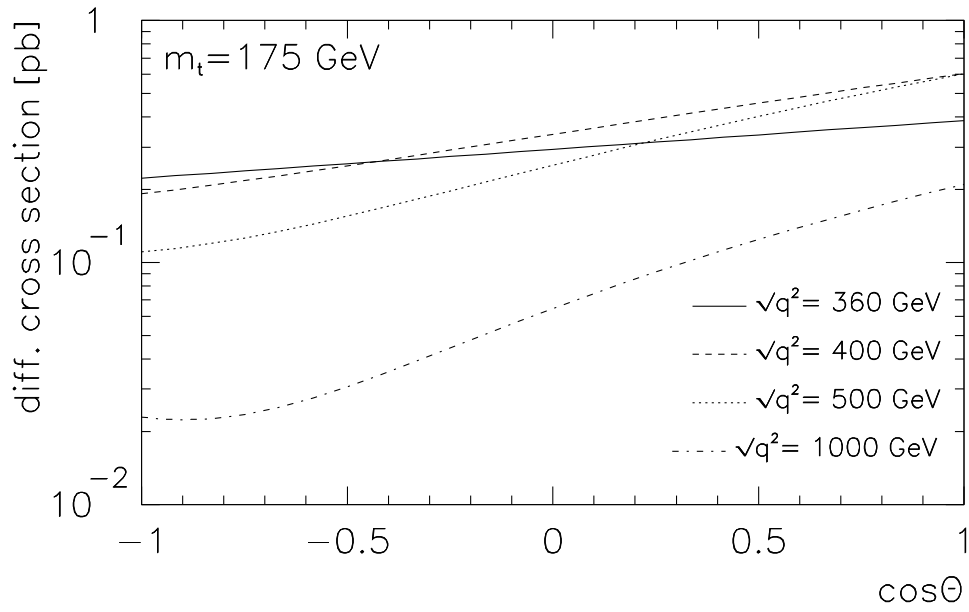.

Figure 5: $O(\alpha_s)$ polar angle distribution of the production rate in $e^+e^- \to t\bar{t}$ at $\sqrt{q^2} = 360$, 400, 500, and 1000 GeV

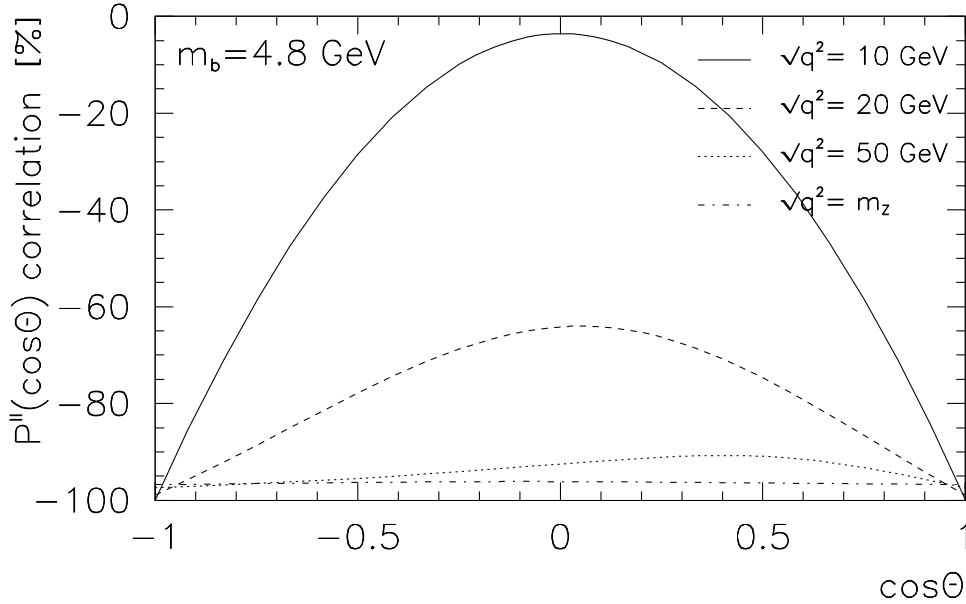Figure 6: Polar angle dependence of the longitudinal spin-spin asymmetry in $e^+e^- \to b\bar{b}$ at $\sqrt{q^2} = 10$, 20 and $50\,\mathrm{GeV}$ and on the Z peak

of the $O(\alpha_s)$ longitudinal spin-spin correlation function $P^{\ell\ell}(\cos\theta)$. The forward-backward asymmetry of $P^{\ell\ell}$ is not as pronounced as in the top quark case and, contrary to the top quark case, its angular distribution is only slightly enhanced in the forward hemisphere. At the Z pole one has an almost flat distribution close to the value of $P^{\ell\ell} = -1$ as expected for massless QCD. The deviation from the -100% value is again due to the anomalous contribution.

In Fig. 7 we exhibit the size of the $O(\alpha_s)$ corrections defined by the measure $\Delta P^{\ell\ell}$ as defined in Eq. (73). Close to threshold at $\sqrt{q^2} = 10\,\mathrm{GeV}$ the $O(\alpha_s)$ corrections in the forward and the backward directions are quite small. The corrections become larger away from the forward and backward directions and rise to $\simeq 3.5\%$ at $\theta = 90^0$. As the energy increases, the $O(\alpha_s)$ corrections become progressively flatter and tend to turn to negative values. At the Z peak the $O(\alpha_s)$ corrections are almost flat and reach a value of $\simeq -3.4\%$ which again shows that they are dominated by the anomalous contribution.

In Fig. 8 we show the $\cos\theta$-dependence of the $(b\bar{b})$-production cross section. The distributions are much flatter than in the top quark pair production case. The differential cross section falls as the center-of-mass energy increases and then reaches back to high values on the Z peak.

9   Summary and conclusion

We have presented analytical results for the $O(\alpha_s)$ corrections to the polar angle dependent longitudinal spin-spin asymmetry $P^{\ell\ell}(\cos\theta)$ in $e^+e^- \to q\bar{q}$. A numerical evaluation of
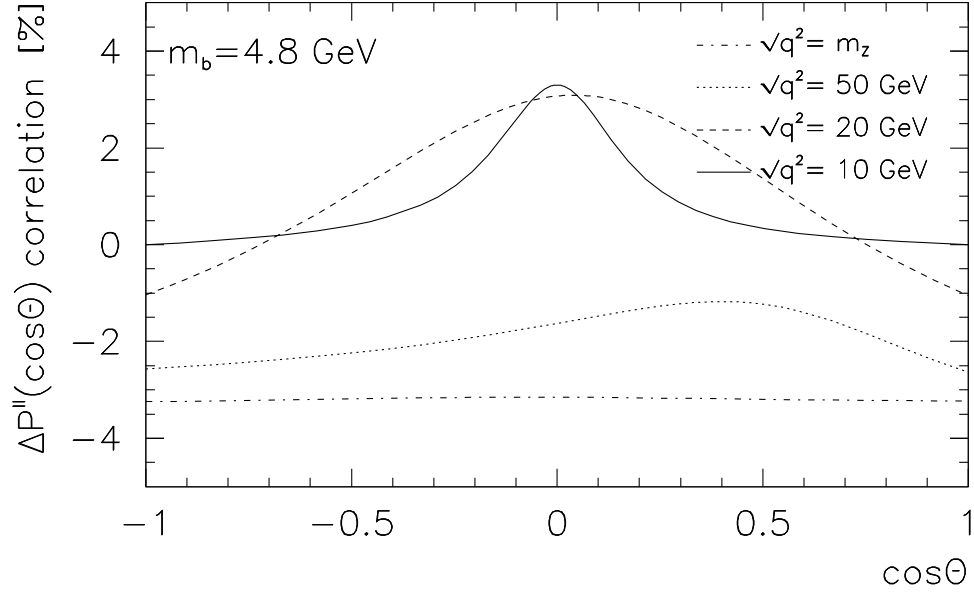
Figure 7: Relative size of $O(\alpha_s)$ corrections to the longitudinal spin-spin asymmetry in $e^+e^- \to b\bar{b}$ at $\sqrt{q^2} = 10$, 20 and 50 GeV and on the Z peak
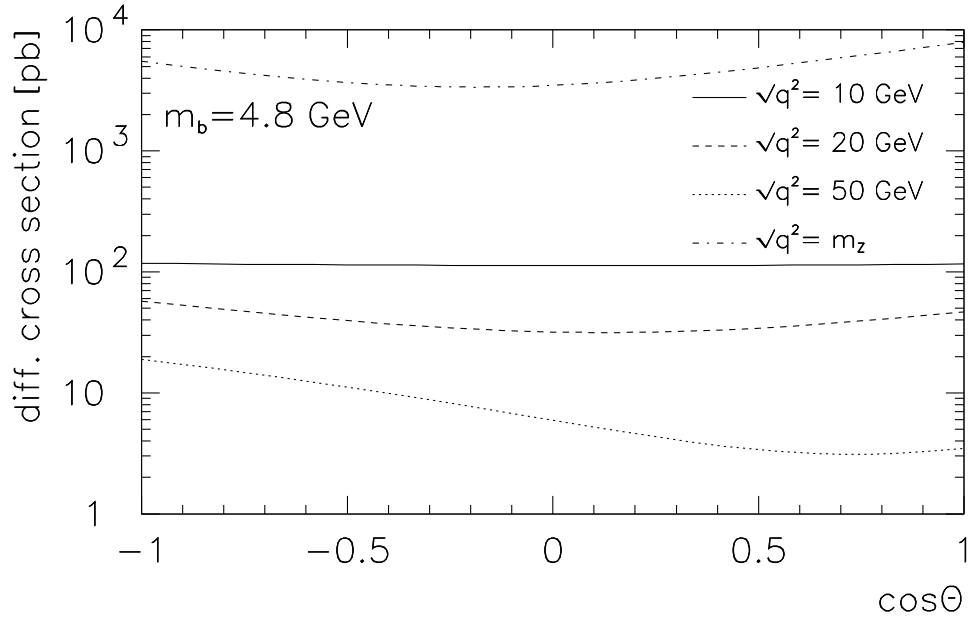

Figure 8: $O(\alpha_s)$ polar angle distribution of the production rate in $e^+e^- \to t\bar{t}$ at $\sqrt{q^2} = 10$, 20 and 50 GeV and on the Z peak

$P^{\ell\ell}(\cos\theta)$ for top quark pair production shows that the $O(\alpha_s)$ corrections are not small and, depending on the energy, can be strongly polar angle dependent. The $O(\alpha_s)$ corrections to $P^{\ell\ell}$ are smaller than the $O(\alpha_s)$ corrections to the cross section itself. The reason is that the $O(\alpha_s)$ corrections to the numerator and the denominator in the (normalized) longitudinal spin-spin asymmetry tend to go in the same direction with the effect that the $O(\alpha_s)$ correction to the ratio becomes reduced. At lower energies the longitudinal spins of the quark and antiquark become almost 100% aligned in the forward and backward direction, i.e. one has $P^{\ell\ell}(\cos\theta = \pm 1) \simeq -1$ with small radiative corrections. As the energy is increased the radiative corrections become larger at the endpoints signalling a slow approach to the asymptotic regime.

For bottom quark pair production on the Z peak one is already close to the asymptotic regime since $m_b^2/m_Z^2 = 2.8 \times 10^{-3}$ (using $m_b = 4.8\,\mathrm{GeV}$, $m_Z = 91.188\,\mathrm{GeV}$ as before). In massless QCD one expects $P^{\ell\ell}(\cos\theta) = -1$ to any order of α_s because there are no spin-flip contributions in massless QCD. This is different in the $m_q \to 0$ (or high energy) limit of QCD where there are residual mass effects starting at $O(\alpha_s)$ which change the naive pattern of massless QCD. In fact, in the high energy limit (or for $m_q \to 0$) one obtains instead $P^{\ell\ell}(\cos\theta) = -1 + 4\alpha_s/3\pi$ due to the anomalous $O(\alpha_s)$ flip and non-flip contributions. The numerical evaluation of the longitudinal spin-spin asymmetry for bottom quark pair production on the Z peak shows that one is already close to the asymptotic form but noticeable preasymptotic effects are still present with respect to the flatness of the $\cos\theta$ distribution and the size of the anomalous contributions. We have discussed in some detail the role of the anomalous contributions and how they contribute to spin-flip and non-flip terms in the three correlation structure functions that determine the $\cos\theta$-dependence of the longitudinal spin-spin asymmetry.

All our results can be applied to QED final state corrections in polarized lepton pair production in $e^+e^- \to \mu^+\mu^-$ and $e^+e^- \to \tau^+\tau^-$. The radiative corrections are, of course, smaller in the QED case due to the smallness of the QED coupling constant α. In particular, in the asymptotic limit, where $P^{\ell\ell}(\cos\theta) = -1 + \alpha/\pi$, the anomalous contribution to the longitudinal spin-spin asymmetry is now only of $O(0.23\%)$.

What remains to be done is to calculate the radiative corrections to the remaining transverse-longitudinal and transverse-transverse spin-spin density matrix elements in the helicity system. Alternatively, one can study the spin-spin density matrix in the off-diagonal basis representation of Ref. [2], which is optimal at the Born term level. Radiative corrections to the spin-spin density matrix in the off-diagonal basis have been considered before using the soft gluon approximation [3]. It is, however, clear that, in the soft gluon approximation, one misses potentially large contributions from e.g. the near-forward emission of hard gluons as described in this paper.

References

[1] W. Bernreuther, J. Phys. **G35** (2008) 083001

[2] S.J. Parke and Y. Shadmi, Phys. Lett. **B387** (1996) 199

[3] Y. Akatsu and O. Terazawa, Int. J. Mod. Phys. **A12** (1997) 2613

[4] H.A. Olsen and J.B. Stav, Phys. Rev. **D56** (1997) 407

[5] M.M. Tung, J. Bernabéu and J. Peñarrocha, Phys. Lett. **B418** (1998) 181

[6] S. Groote, J.G. Körner and J.A. Leyva, Phys. Lett. **B418** (1998) 192

[7] A. Brandenburg, M. Flesch and P. Uwer, Phys. Rev. **D59** (1999) 014001

[8] W. Bernreuther, A. Brandenburg and P. Uwer,
Phys. Rev. Lett. **79** (1997) 189

[9] G. Rodrigo, A. Santamaria and M. S. Bilenky, Phys. Rev. Lett. **79** (1997) 193

[10] P. Nason and C. Oleari, Phys. Lett. **B407** (1997) 57

[11] S. Groote, J.G. Körner and J.A. Leyva,
Phys. Rev. **D56** (1997) 6031; Eur. Phys. J. **C7** (1999) 49

[12] G. Grunberg, Y.J. Ng and S.H.H. Tye, Phys. Rev. **D21** (1980) 62

[13] J.G. Körner, A. Pilaftsis and M.M. Tung, Z. Phys. **C63** (1994) 575

[14] S. Groote, J.G. Körner and M.M. Tung, Z. Phys. **C74** (1997) 615

[15] T.D. Lee and M. Nauenberg, Phys. Rev. **133** (1964) B1549; R. Kleiss, Z. Phys. **C33** (1987) 433; S. Jadach, J.H. Kühn, R.G. Stuart and Z. Was, Z. Phys. **C38** (1988) 609 [Erratum-ibid. **C45** (1990) 528]; H.F. Contopanagos and M.B. Einhorn, Phys. Lett. **B277** (1992) 345; Nucl. Phys. **B377** (1992) 20; S. Dittmaier and A. Kaiser, Phys. Rev. **D65** (2002) 113003

[16] A.V. Smilga, Comments Nucl. Part. Phys. **20** (1991) 69

[17] Z. Was, Acta Phys. Polon. **B18** (1987) 1099

[18] B. Falk and L.M. Sehgal, Phys. Lett. **B325** (1994) 509

[19] M. Fischer, S. Groote, J.G. Körner and M.C. Mauser, Phys. Rev. **D67** (2003) 113008

[20] L. Trentadue and M. Verbeni, Nucl. Phys. **B583** (2000) 307; Phys. Lett. **B478** (2000) 137; L.M. Sehgal, Phys. Lett. **B569** (2003) 25; V.S. Schulz and L.M. Sehgal, Phys. Lett. **B594** (2004) 153; E. Gabrielli and L. Trentadue, Nucl. Phys. **B792** (2008) 48

[21] S. Groote, W. S. Huo, A. Kadeer and J. G. Körner, Phys. Rev. **D76** (2007) 014012

[22] M.M. Tung, J. Bernabéu and J. Peñarrocha, Nucl. Phys. **B470** (1996) 41

[23] J. Kodaira, T. Nasuno and S.J. Parke, Phys. Rev. **D59** (1999) 014023

[24] S. Groote, J.G. Körner and M.M. Tung, Z. Phys. **C70** (1996) 281

[25] V. Ravindran and W.L. van Neerven, Nucl. Phys. **B589** (2000) 507

[26] C. Amsler *et al.* [Particle Data Group], Phys. Lett. **B667** (2008) 1

[27] S. Groote and J.G. Körner, Report No. MZ-TH/08-39 [arXiv:0811.2728 [hep-ph]]

[28] S. Groote, J.G. Körner and J.A. Leyva, Nucl. Phys. **B527** (1998) 3

[29] A.D. Dolgov and V.I. Zakharov, Nucl. Phys. **B27** (1971) 525; J. Hořejši, Phys. Rev. **D32** (1985) 1029; J. Hořejši and O. Teryaev, Z. Phys. **C65** (1995) 691

[30] M. Fischer, S. Groote, J.G. Körner, M.C. Mauser and B. Lampe, Phys. Lett. **B451** (1999) 406; M. Fischer, S. Groote, J.G. Körner and M.C. Mauser, Phys. Rev. **D63** (2001) 031501; Phys. Rev. **D65** (2002) 054036; H.S. Do, S. Groote, J.G. Körner and M.C. Mauser, Phys. Rev. **D67** (2003) 091501